A. P. Alexandrov
RESEARCH INSTITUTE
OF TECHNOLOGY
N I T I

Phase diagrams for multicomponent systems containing corium and products of its interaction with NPP materials (CORPHAD) Phase 2

Progress report
01/07/03 – 30/06/04

Phase relation study in the system $Fe_2O_3(Fe_3O_4)$ – SiO_2 at different oxygen partial pressures

Project	Generation of data for phase diagrams of multi-component oxidic mixtures, based on prototypic molten corium (CORPHAD, phase 2), #1950.2
Customer	ISTC
File specification	CORPHAD2/RCP-0403
Prepared by	A. P. Alexandrov Research Institute of Technology. (NITI) Russia, 188540, Sosnovy Bor, Leningrad Region, NITI
Project Manager	Name: Yu. Aniskevich Signature: Date: October, 2004

Authors

Professor	V.B. Khabensky
Doctor	S.V. Bechta
Doctor	V.S. Granovsky
Academician	V.V. Gusarov
	S.A. Vitol
	E.V. Krushinov
Professor	Yu.B. Petrov
Doctor	S.Ju. Kotova
Doctor	A. A. Sulatskey
Doctor	I.V. Kulagin
Doctor	D.B. Lopukh
Doctor	A.Yu. Pechenkov
Doctor	L.P. Mezentseva
Doctor	A.V. Merzlyakov
	V.G. Blizniuk
	V.R. Bulighin
	E.M. Beliaeva
	E.K. Kaliago
	N.E. Kamensky
	A.V. Lisenko
	A.P. Martinov
	V.V. Martinov
	E.V. Shevchenko
	A.A. Chertkov
	V.I. Almjashev
	S.K. Kuchaeva
	N.A. Lomanova
	V.F. Popova

ABSTRACT

The results of an investigation on Fe_2O_3 – SiO_2 system in air and in oxygen and Fe_3O_4 – SiO_2 system in inert atmosphere are presented in the report of the ISTC «CORPHAD» project (phase 2). Visual polythermal analysis (high temperature microscope and Galakhov microfurnace) and differential thermal analysis (DTA) were used in the study. X-ray powder diffraction study and SEM/EDX analysis were used for interaction products investigation in the systems.

Phase relations in the systems were investigated and corresponding phase diagrams were constructed depending on oxygen partial pressure. Eutectic points (temperature and concentration) and miscibility gap regions were determined.

In Fe_2O_3 – SiO_2 system eutectic point was at 1440°C and 88±1 mass % Fe_2O_3 (in air and in oxygen). The region of miscibility gap extended from 78/80 to ~ 20/10 mass % Fe_2O_3.

It was established that an additional component (Fe_3O_4) appeared in Fe_2O_3 – SiO_2 system at temperatures higher then decomposition temperature of Fe_2O_3 into Fe_3O_4 (1375 in air and 1430°C in oxygen atmosphere). Due to incomplete decomposing process the system should be represented as $Fe_2O_3(Fe_3O_4)$ – SiO_2. At the same time figurative points of the compositions shifted into the ternary Fe_2O_3 – FeO – SiO_2 diagram forming the polythermal section line mismatching however with the polythermal section line of Fe_3O_4 – SiO_2.

In Fe_3O_4 – SiO_2 system (inert atmosphere) eutectic point corresponded to 1440°C and 79±1 mass % Fe_3O_4. The region of miscibility gap extended from 70 to 30-25 mass % Fe_3O_4. Microphotos of quenched samples confirming phase diagram construction are presented as well as SEM/EDX results permitting to represent coexistence curve are given.

It was shown that the both diagrams (Fe_2O_3 – SiO_2 and Fe_3O_4 – SiO_2) are similar but not identical due to the incomplete Fe_2O_3 decomposition into Fe_3O_4 at temperatures higher than 1375°C and to reversibility of the process.

Content

1. Introduction

At the ex-vessel stage of NPP severe accidents melt corium can contain a significant quantity of iron oxides as products of steel oxidizing and silica as a product of corium interaction with concretes, sacrificial material and refectories. At this accident stage a melt corium pool is for a long time in oxidizing conditions caused by steam-air atmosphere.

The circumstances mentioned above initialized the study of systems contained iron oxides and silica at high oxygen partial pressure to optimize the databases available and to prove the calculation codes.

According to the working plan of the ISTC «CORPHAD» project (phase 2), phase relations in the $Fe_2O_3(Fe_3O_4)$ – SiO_2 system have been investigated at different oxygen partial pressures.

Phase diagram studies of silicate systems, where iron is one of the components, are complicated by the fact that iron readily occurs in three different states of oxidation: Fe^{3+}, Fe^{2+} and Fe^0 (trivalent, divalent and metallic). Therefore, the equilibrium composition of condensed phases varies with the gas composition. Due to this circumstance, we have undertaken an experiment at various oxygen partial pressures.

We have investigated two systems, namely hematite – silica (Fe_2O_3 – SiO_2) in oxygen atmosphere and in air, and the system magnetite – silica (Fe_3O_4 – SiO_2) in inert atmosphere.

There is not much reliable data on phase equilibria in these systems and there are no phase diagrams available in literature in spite of such investigations were carried out in the middle of the last century [1-4]. The most well-known and thoroughly investigated is ternary FeO – Fe_2O_3 – SiO_2 system (Fig. 1) by Arnulf Muan [3]. The ternary eutectic point corresponding to 16 FeO – 69 Fe_2O_3 – 15 SiO_2 (mass %) at ~1455°C was predicted in this work.

However, there is not data in this work related to ferric oxide corner and phase equilibrium in Fe_2O_3 – SiO_2 system.

Therefore, the objectives of the research were to study phase relations in Fe_2O_3 - SiO_2 system and its fusion diagram construction including temperature and concentration of eutectic point determination.

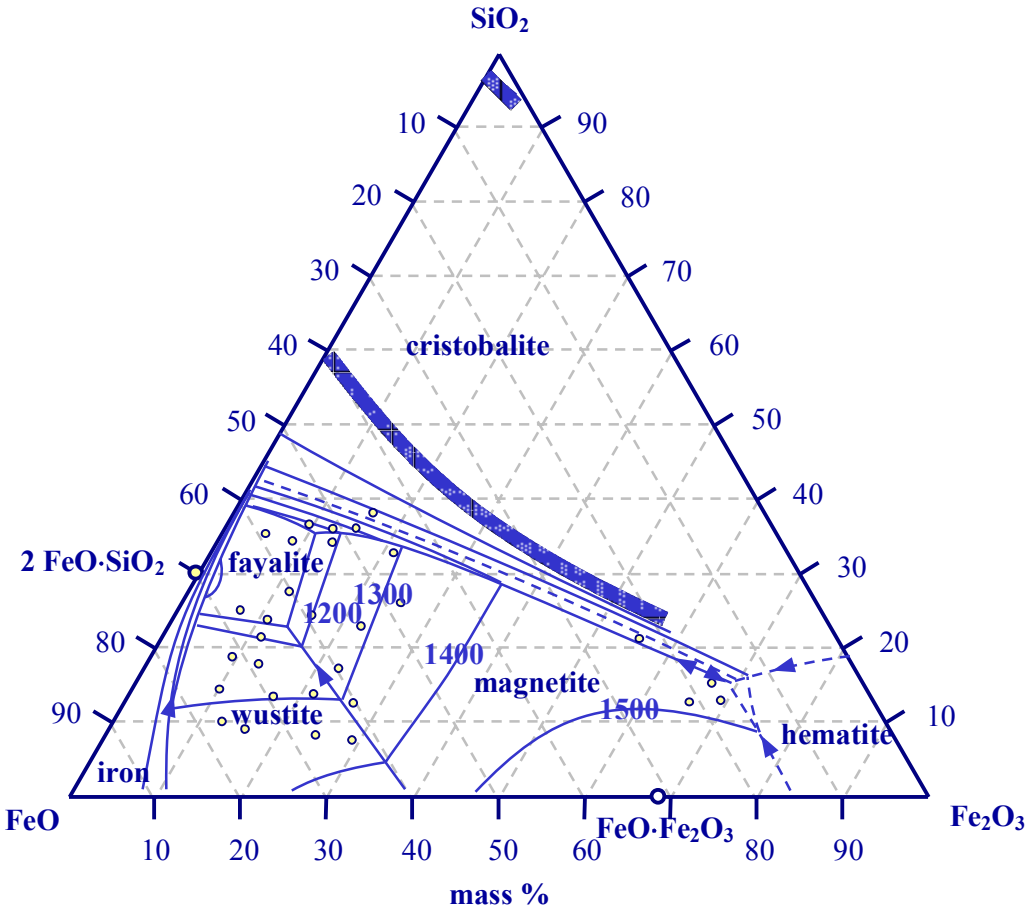

Fig. 1. Fusion diagram for the system FeO – Fe_2O_3 – SiO_2 by A. Muan (mainly in reducing atmosphere) [3]

2. Experimental part

2.1. Materials, preparation techniques and methods of investigation

Starting materials for hematite – silica system (Fe_2O_3 – SiO_2) were chemicals of the highest purity available:

- 99.97% for Fe_2O_3;
- 99.99% for SiO_2 (Brasilian rock crystal);
- 99.99% for Fe (carbonyl iron).

Ferric oxide was preliminary dried at 300°C and silica at 110°C for 3 hr.

Starting materials in the case of Fe_3O_4 – SiO_2 system were Fe_3O_4, e.g. ferric-ferrous oxide

or magnetite, and silica. Magnetite (Fe_3O_4) as a precursor was prepared by the following reaction:

$$Fe_2O_3 + Fe \rightarrow Fe_3O_4,$$

where Fe is a carbonyl iron, at 1300°C in argon flow for 1 hr in corundum crucible.
Synthesis of samples in both systems was carried out by solid state reaction; initial compositions pretreatment was carried on in air in kilns with silit heaters.

After heat treatment products were analyzed by X-ray powder diffraction with Co-radiation (DRON-3), DTA using of differential scanning calorimeter (DSC, Netzsch, Simultaneous Thermal Analyser STA 429) and high temperature thermal analyzer (VTA, Ukrain). Conditions of the DTA (DSC) experiment were the same for all specimens:

- Pt crucibles;
- 30 mg specimen;
- 10 °/min heating rate;
- air or oxygen.

VTA experiment was carried on at 40 °/min heating rate in Al_2O_3 crucibles.

Solidus-liquidus temperature determination was realized by visual polythermal analysis (VPA), using of unique devices - high-temperature microscope [5] and Galakhov microfurnace [6] developed and constructed in the Institute of Silicate Chemistry RAS. Their descriptions are given in sections 2.2. and 2.3.

The powdered samples (10 g) prepared in $Fe_2O_3 – SiO_2$ system were used then (~0.4 mg) for solidus-liquidus determination by high-temperature microscope.

In Galakhov microfurnace pieces (~3×3×1 mm, i.e. ~7.5 mg) of broken tablets were used for the experiments. These pieces were set between spiral coils of the holder (~2 mm in diameter) and placed in the isothermal zone of the microfurnace. Besides, the quenching of the samples of $Fe_3O_4 – SiO_2$ system was performed in Galakhov microfurnace with the subsequent determination of their microstructure and element content by scanning electron microscopy (SEM) and energy dispersed X-ray analysis (EDX) using ABT-55 (Japan) electron microscope with microprobe analyzer Link_AN_10000/S85 (Great Britain). All these investigations were an additional basis for fusion diagram of $Fe_3O_4 – SiO_2$ system construction.

Spectral characteristics were obtained for every specimen selected for SEM/EDX analysis. According these characteristics a total element and phase content were determined.

Quantitative analysis was done by comparing spectral intensity of standard (particularly pure, specially prepared) substances and that of the specimen under investigation. The standards used (U, Zr, Cr, Fe, Si, Ca, Ni) were the part of the complete set supplied by Link. The oxygen amount was determined by deficiency of the total intensity. Calibration was made according to total intensity of copper spectrum.

The limit of the reliable determination of an element content depends on its ordinal number in the Periodic Table and varies from 0.1 mass % for light elements up to 0.3 mass % for the heavy ones. Detection of smaller amounts is unreliable. Oxygen content was determined by the specimen's mass deficiency, with permissible limit not exceeding 4 % mass.

2.2. The Fe_2O_3 – SiO_2 system study in air and in oxygen atmosphere

Ten gram-samples were made up by mixing these materials in following proportions:

Table 1

Starting compositions in Fe_2O_3 – SiO_2 system

Sample number	Content			
	Fe_2O_3		SiO_2	
	mol %	mass %	mol %	mass %
1	90.00	96	10.00	4
11	83.33	93	16.67	7
2	82.00	92	18.00	8
3	80.00	91	20.00	9
4	78.00	90	22.00	10
12	75.32	89	24.68	11
13	73.40	88	26.60	12
14	71.57	87	28.43	13
5	70.00	86	30.00	14
6	60.00	80	40.00	20
7	50.00	73	50.00	27
8	40.00	64	60.00	36
9	20.00	40	80.00	60
10	10.00	23	90.00	77
15	9.09	21	90.91	79
16	8.60	20	91.40	80
17	7.63	18	92.37	82
18	6.69	16	93.31	84
19	5.77	14	94.23	86

For better homogenization mixtures were ground under alcohol for about 3 hr, pressed into tablets and stepwise preheated in air in the temperature range 1000-1300°C during 5 hr with intermittent grindings.

X-ray analysis has indicated that at 1000 and 1100°C the mixture had the composition of α-Fe_2O_3 and SiO_2 (quartz), and at 1200 and 1300°C – it was α -Fe_2O_3 and SiO_2 (quartz and cristobalite) (Fig. 2, 3).

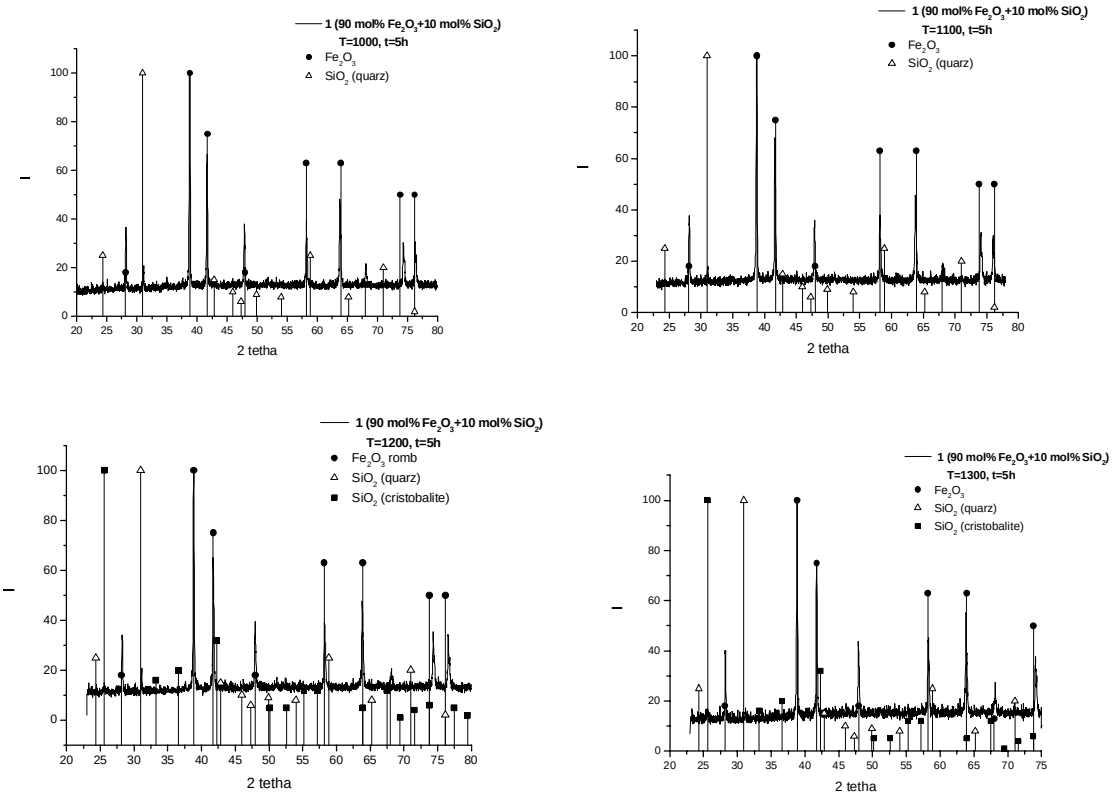

Fig. 2.X-ray diffraction patterns of powdered sample 96 mass % Fe_2O_3 at different heat treatment temperatures – 1000, 1100, 1200 и 1300 °C

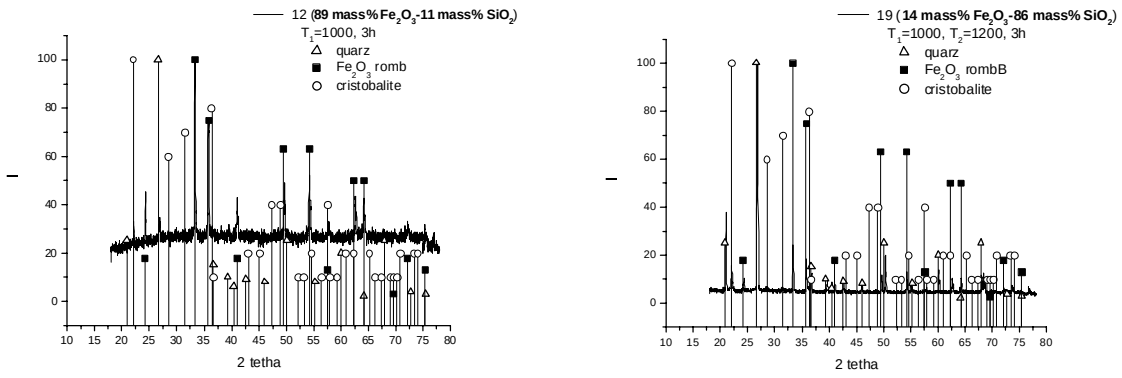

Fig. 3. X-ray diffraction patterns of powdered samples: 89 mass % Fe_2O_3 (sample N 12) and 14 mass % Fe_2O_3 (sample N 19) at 1200°C

The powdered samples prepared then were used for solidus-liquidus determination by high-temperature microscope [5]. This device is schematically presented in Fig. 4.

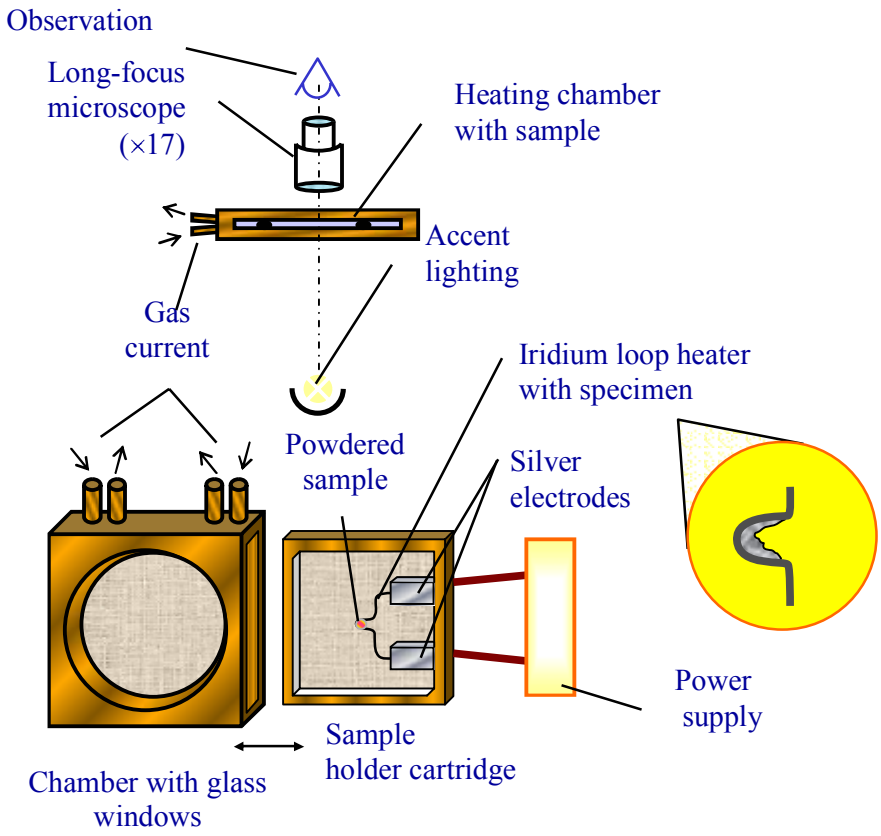

Fig. 4. Scheme of high-temperature microscope

The main part of the device is an optical microscope itself adjusted for determining of melting point of powdered samples. Instead of object (the place under the objective) the optical microscope is fitted with heating chamber, which could be used in different atmospheres. Heating element is iridium wire loop calibrated against voltage values at melting points of standards (Table 2).

Table 2

Standards for the calibration of the heating element

Solids	K_2SO_4	$CaO \cdot Al_2O_3$	$SiO_2 \cdot Al_2O_3$	Al_2O_3	Fe_2O_3*	SiO_2
Temperature, °C	1069	1600	1910	2054	1539	1723

* - in oxygen

But in the present experiments due to high viscosity of melts in the system, we have used IVTANTHERMO [7] melting points of initial components, e.g. Fe_2O_3 and SiO_2 (Table 2), to calibrate the heating element.

Solidus-liquidus determination was carried out in air and in oxygen flow. The partial oxygen pressure in this case was about 0.21 and one atmosphere respectively. The experimental error of these measurements was typically within ±25°C, but it can be higher for viscose melts.

Besides, the overcoming of the determined temperature can take place due to high heating rate (~1000°C/s). To avoid this effect heating process was carried on stepwise with ~10 s exposition every other 500°C. Solidus temperature was fixed by slightly moving of the specimen to the top of the loop or to its site as a result of first portion of melt formation. Liquidus temperature was fixed by the moment of drop of melt formation. In the case of high silica content (high melt viscosity) – by the moment when the drop of melt became transparent.

Data obtained for solidus-liquidus temperature in the Fe_2O_3 – SiO_2 system in air and in oxygen flow were identical, and they are presented for all nineteen initial compositions in Table 3 and as a fusion diagram of the Fe_2O_3 – SiO_2 system in Fig. 5. The diagram is given in coordinates "nominal composition – temperature"

Table 3

Solidus-liquidus temperature in the Fe_2O_3 – SiO_2 system in air and in oxygen (high temperature microscope)

Fe_2O_3 content		**Temperature, °C***		
mol % (±0.03%)	**mass % (±0.01%)**	**solidus**	**liquidus**	**monotectic**
100			1539	
90.00	96	1470	1517	
83.33	93	1470	1505	
82.00	92	1470	1490	
78.00	90	1470	1470	
75.32	89	-	1475	
73.40	88	1470	1490	
71.57	87	1470	1505	
70.00	86	1470	-	1539
60.00	80		-	1530
50.00	73		-	1530
40.00	64		-	1530
20.00	40		-	1530
10.00	23		-	-
9.09	21		-	1538
8.60	20		-	1538
7.63	18		1655	-
6.69	16		1655	-
5.77	14		-	-
0			1723	

* - an experimental error of these measurements is ± 25°C.

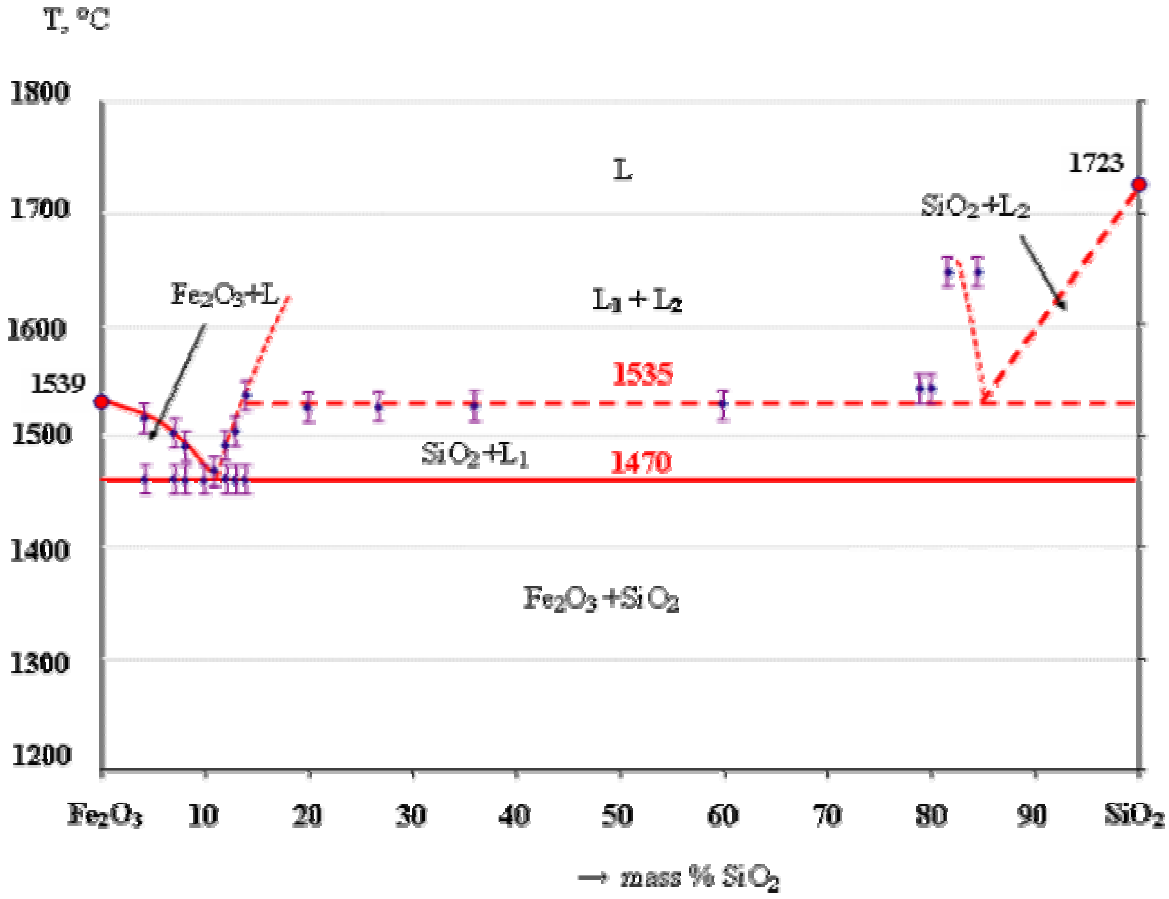

Fig. 5. Fusion diagram of the Fe_2O_3 – SiO_2 system (high temperature microscope, air and oxygen); ● - IVTANTHERMO

It is a simple diagram with one eutectic point at ~1470°C and 89±1 mass % of Fe_2O_3. The region of miscibility gap was determined according the knuckle line of liquidus and monotectic location. It extended from 78/80 to about 20/10 mass % Fe_2O_3.

In spite of the fact that the experiments were carried out not only in air but in oxidizing atmosphere too, the presence of ferrous oxide (wustite) in the system at high temperatures was evident [8, 9]. That was confirmed by the DTA results obtained in air (p_{O_2}=0.21 atm). They are given in Fig. 6 for samples having the compositions in the concentration region near eutectic point.

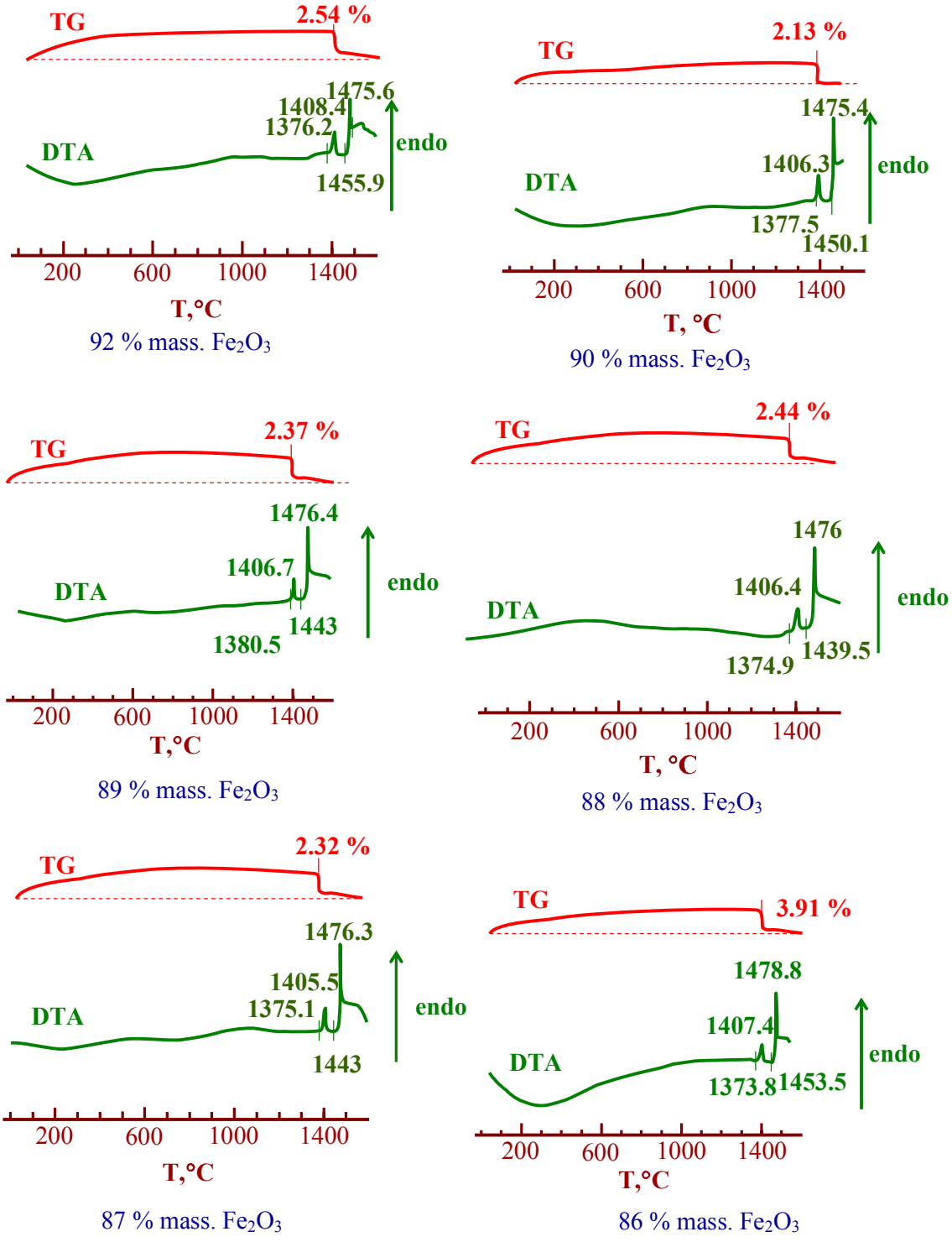

Fig. 6. DTA and TG curves for the samples in Fe_2O_3 – SiO_2 system (in air)

Each DTA curve exhibits two endothermic effects at temperatures near 1380 and 1440°C (Table 4). The first effect followed by mass loss corresponds in our opinion to Fe_2O_3 decomposition into Fe_3O_4; the second one – to eutectic melting.

Table 4

DTA results of samples in Fe_2O_3 – SiO_2 system in air and in oxygen

Sample content (mass %)	Temperature, °C			
	I effect		II effect	
	onset	max	onset	max
92 Fe_2O_3 - 8 SiO_2	1376	1408	1456	1476
90 Fe_2O_3 - 10 SiO_2	1387	1408	1457	1476
89 Fe_2O_3 - 11 SiO_2	1380	1406	1443	1476
88 Fe_2O_3 - 12 SiO_2	1375	1406	1440	1476
87 Fe_2O_3 - 13 SiO_2	1375	1406	1443	1476
86 Fe_2O_3 - 14 SiO_2	1374	1407	1454	1479
92 Fe_2O_3 - 8 SiO_2*	1430	1451	1459	1475

* – in oxygen

Eutectic temperature determined by DTA in air (~1440°C) is very close to that determined by high-temperature microscope (1470±25°C).

Similar experiment was carried out in oxygen (p_{O_2}~1 atm) to establish the influence of oxygen on these effects (Fig. 7).

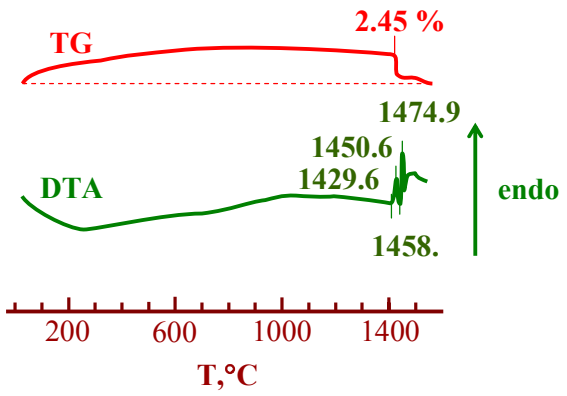

Fig. 7. DTA and TG curves for the sample 92 mass % Fe_2O_3 in Fe_2O_3 – SiO_2 system (oxygen atmosphere, p_{O_2}~1 atm)

As we can see the influence of oxygen is in the displacement of the first endothermic effect corresponding to the Fe_2O_3 decomposition into Fe_3O_4 to a higher temperature range by ~50°C (Fig. 6, 7 and Table 4). Whereas the second effect corresponding to the eutectic melting is unchanged. Thus in oxygen the decomposing process is observed in any case but at higher temperature.

To check it an experiment on Fe_2O_3 decomposition was carried out in Pt crucible at 1450°C in air for 1 hr. The experiment has shown that at these conditions the weight loss was 2.93% compared to initial mass (0.543 g) and the final product of heat treatment was a mixture of Fe_2O_3 and Fe_3O_4 (Fig. 8).

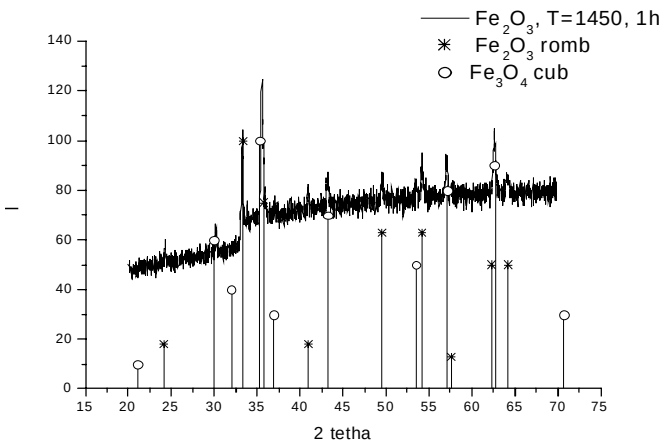

Fig. 8. X-ray diffraction pattern of powdered Fe_2O_3 after heating at 1450°C in air for 1 hr (Pt crucible)

According to all these results obtained (VPA and DTA (DSC)) a fusion diagrams of the system $Fe_2O_3(Fe_3O_4)$ – SiO_2 at different oxygen partial pressure (p_{O_2}=0.21 and ~1 atm) can be presented as follows (Fig. 9, 10).

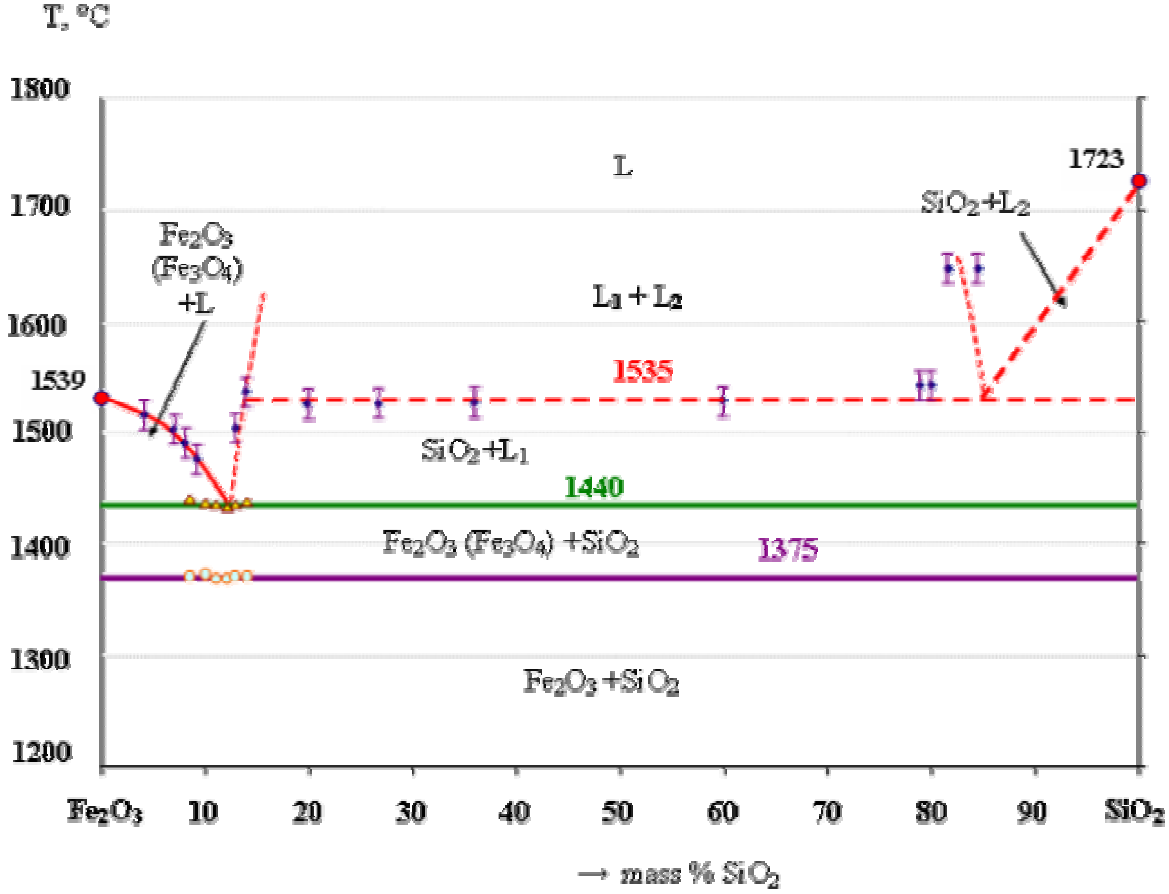

Fig. 9. Fusion diagram of the system Fe_2O_3 – SiO_2 in air (pO_2=0.21) according to VPA and DTA (DSC): ◆ and red line – high temperature microscope data; ▲ and green line – DTA (DSC) data; ○ and violet line – temperature of Fe_2O_3 decomposition into Fe_3O_4 determined by DTA (DSC); ● - IVTANTHERMO

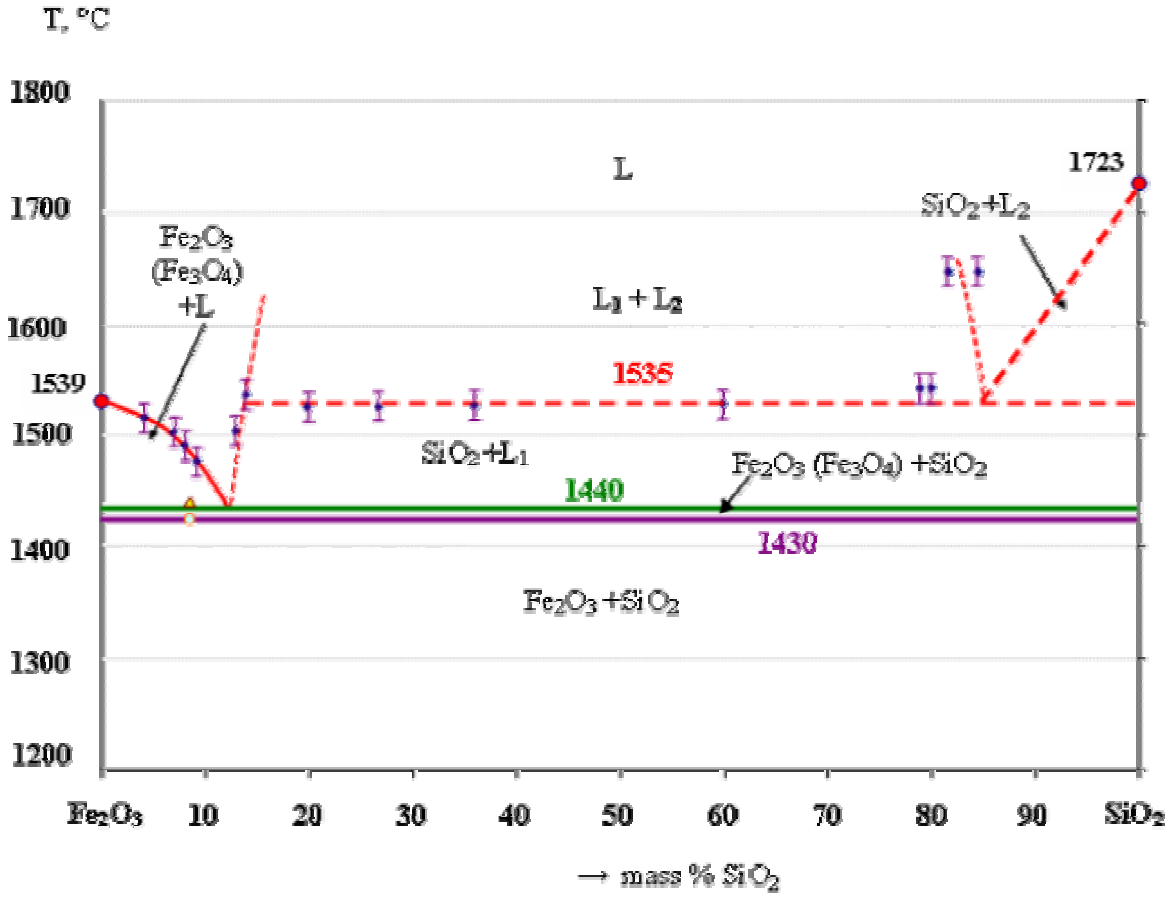

Fig. 10. Fusion diagram of the system Fe_2O_3 – SiO_2 in oxygen (pO_2~1 atm) according to VPA and DTA (DSC): ◆ and red line – high temperature microscope data; △ and green line – DTA (DSC) data; ○ and violet line – temperature of Fe_2O_3 decomposition into Fe_3O_4 determined by DTA (DSC) ; ● - IVTANTHERMO

Taking the process of Fe_2O_3 decomposition into Fe_3O_4 at temperatures higher than 1375°C (in air) and higher than 1430°C (in oxygen) into account the necessity of studying the Fe_3O_4 – SiO_2 becomes obvious.

2.3. The Fe_3O_4 – SiO_2 system study in inert atmosphere

The research was undertaken in inert atmosphere (p_{O_2}~10^{-8}), namely in argon and helium of highest commercially-available quality.

In the Fe_3O_4 – SiO_2 system twelve compositions were prepared by solid state technique. Charge compositions are listed in Table 5.

Table 5

Charge compositions in Fe_3O_4 - SiO_2 system

Sample number	Content			
	Fe_3O_4		SiO_2	
	mol %	mass %	mol %	mass %
1	90	97.20	10	2.80
2	80	93.91	20	6.09
3	70	89.99	30	10.01
4	60	85.25	40	14.75
5	50	79.39	50	20.61
6	65	87.74	35	12.26
7	40	71.98	60	28.02
8	30	62.28	70	37.72
9	20	49.06	80	50.94
10	10	29.98	90	70.02
11	5	16.86	95	83.14
12	3	11.16	97	88.84
13	1	3.75	99	96.25

Tablets of mixtures prepared were preheated at 1300°C in argon flow for 1 hr.

X-ray analysis of samples has indicated (Fig. 11) a presence of cubic Fe_3O_4 and silica as quartz and cristobalite.

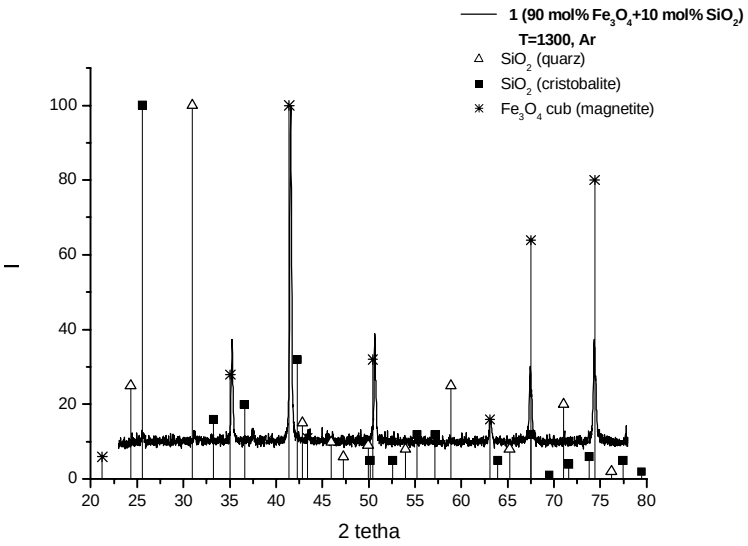

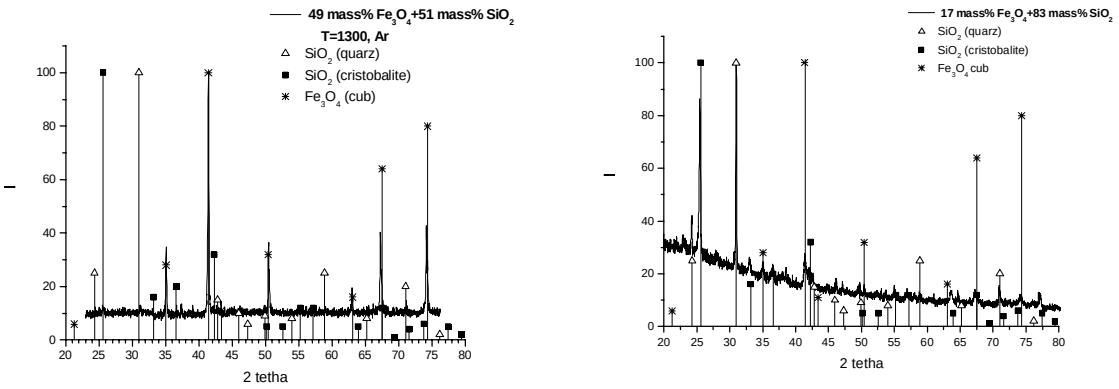

Fig. 11. X-ray diffraction patterns of powdered samples 97 mass % Fe_3O_4 (sample 1); 49 mass % Fe_3O_4 (sample 9) and 17 mass % Fe_3O_4 (sample 11) at 1300°C

Solidus-liquidus temperature determination in inert atmosphere was carried out in Galakhov microfurnace [6] (Fig. 12).

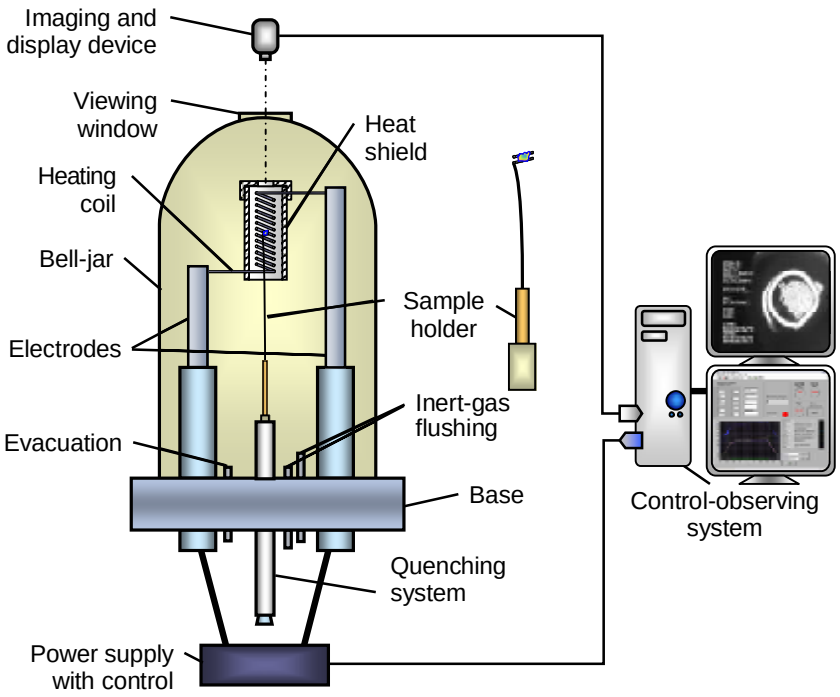

Fig. 12. Scheme of Galakhov microfurnace

The tungsten heating spirals was calibrated against power values at melting points of standards mainly metals, presented in Table 6.

Table 6

Standards for the heating elements calibration

Solids	Ag	Au	Pd	Pt	Rh	Al_2O_3
Temperature, °C	962	1063	1554	1769	1964	2054

Microfurnace design permitted a strong sample quenching.

Liquidus temperature was fixed by the moment of melt spreading over the wire holder surface.

There are at least four arguments for this measurement technique:

- heating up to the melt appearance is carried out very quickly (~ 10 s);
- a sample is prepared in such a way to obtain a skeleton structure of refractory phase (). Hence the sample prepared begins to spread only at skeleton destructing. It takes place only in the case, when solid phase quantity does not exceed 5 vol. %.
- a strong quenching is carried out by throw down of the sample from the heating zone. Quenched sample microstructure investigation usually shows the absence of unfused domains, that is an evidence of complete melting;
- VPA data are confirmed by DTA, which is regarding as classic method of phase diagram study, and by results obtained by other methods, in particular VPA IMCC.

Solidus temperature was fixed by the moment of geometric form degradation of the sample at heating. Usually this process is well observed by monitor at proper magnification.

Working temperature range was kept within 1300-2300°C. An experimental error was ±25°C. Working atmosphere was gaseous helium of 99.99% purity at pressure about 0.25 atm.

For accuracy testing of measurements in Galakhov microfurnace an initial sample of Fe_3O_4 was melted down (melting temperature based on IVTANTHERMO is 1597°C [7]). At using a standard molybdenum holder sample of Fe_3O_4 was melted down at 1451°C. In this case a strong interaction between a sample and a holder was observed (Fig. 13).

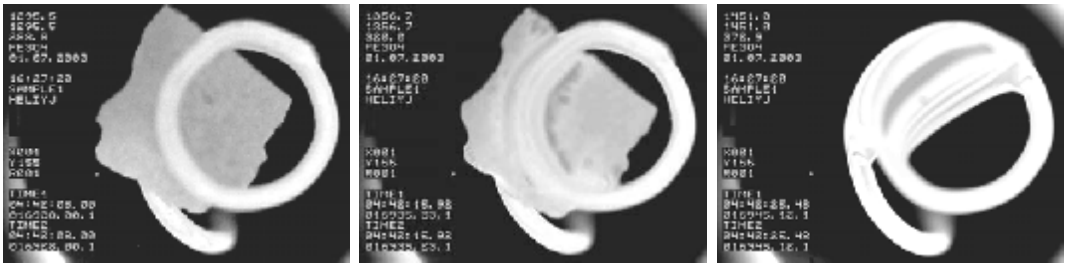

1 2 3

Fig. 13. A sample of Fe_3O_4 in the experiment (molybdenum holder): 1 – before interaction (T=1295.5°C); 2 – the beginning of interaction with molybdenum holder (T=1356.7°C); 3 – complete melting (T=1451°C)

In order to avoid the interaction with molybdenum holder we used molybdenum holder coved with ZrC_4 but the result was not satisfied. The sample of Fe_3O_4 interacted with the holder and melted down at 1433°C (Fig. 14).

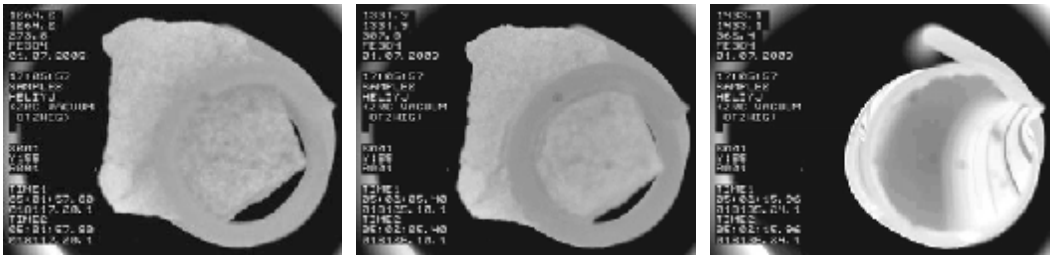

1 2 3

Fig. 14. A sample of Fe_3O_4 in the experiment (molybdenum holder coved with ZrC_4): 1 – before interaction (T=1264.2°C); 2 – the beginning of interaction with the holder (T=1331.9°C); 3 – complete melting (T=1433.1°C)

The best result was obtained when iridium holder was used. No interaction was observed (Fig. 15), and complete melting of the sample was observed at 1614°C that was in a good agreement with value available in literature for Fe_3O_4 [7].

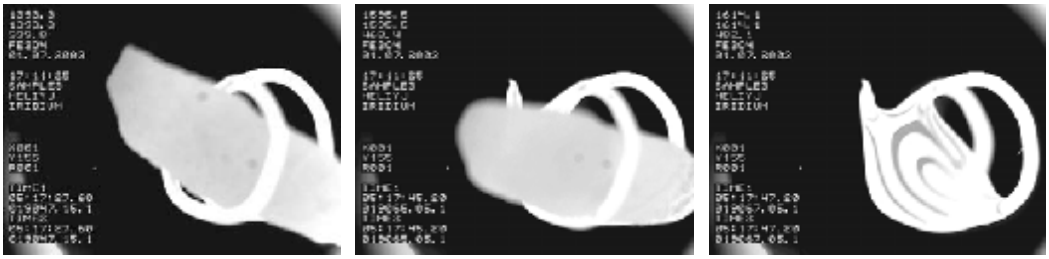

1 2 3

Fig. 15. A sample of Fe_3O_4 in the experiment (iridium holder): 1 – before interaction (T=1393.3°C); 2 – the beginning of interaction with the holder (T=1595.5°C); 3 – complete melting (T=1614.1°C)

Thus, during experiments in Galakhov microfurnace iridium holder was used. All results on liquidus-solidus temperature measurements are presented in Table 7 and as a fusion diagram in Fig. 16.

Table 7

Solidus-liquidus temperature in the Fe_3O_4 – SiO_2 system (Galakhov microfurnace data, inert atmosphere, p_{O_2}~10^{-8})

Fe_3O_4 content		Temperature, °C*		
mol % (±0.03%)	**mass % (±0.01%)**	**solidus**	**liquidus**	**monotectic**
90	97	1449	1561	
80	94	-	1548	
70	90	1441	1511	
65	88	1445	1470	
60	85	1446	1540	
50	79	1448	-	
40	72	1424	-	1560
30	62	-	-	1581
20	49	1429	-	1589
10	30	1434	-	1556
5	17	1440	1681	
3	11	-	1681	
1	5	-	1701	

* - an experimental error of these measurements is ± 30°C.

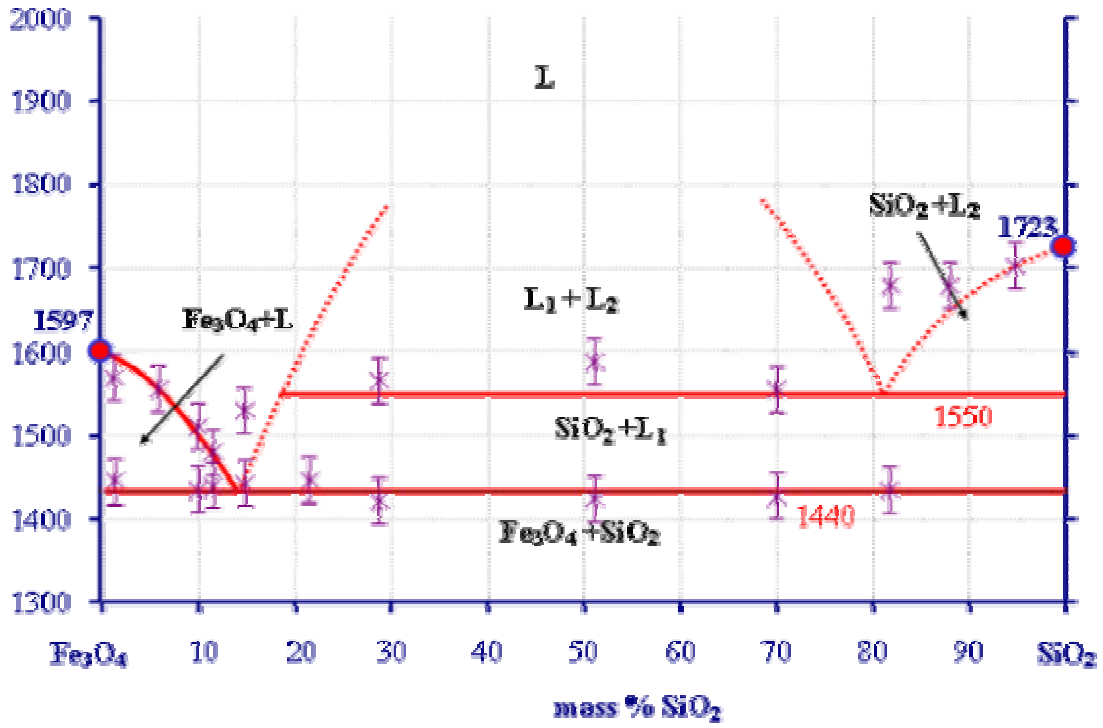

Fig. 16. Fusion diagram of the Fe_3O_4 - SiO_2 system in the inert atmosphere (Galakhov microfurnace, p_{O_2}≈10^{-8})

According to VPA this is a diagram with one eutectic point at 1440°C and ~85 mass % Fe_3O_4. The region of miscibility gap extends presumably from 80 to 20 mass % Fe_3O_4.

DTA indicates two endothermic effects (Fig. 13): the first one at 1470°C corresponds to

eutectic melting, the second one - to monotectic melting.

Subsequent complex analysis of the samples obtained by quenching from different temperatures in Galakhov microfurnace permitted to refine liquidus temperatures, eutectic point position and to determine an approximate coexistence curve location in the fusion diagram of the Fe_3O_4 – SiO_2 system. For this purpose element content and microstructure analysis was carried out. Microstructure analysis usually gives an opportunity to establish the prior crystalline form at cooling process below liquidus temperatures.

The samples during experiments, measurement results obtained by microstructure analysis and SEM/EDX investigations in the Fe_3O_4 – SiO_2 system are presented in Fig. 17-52 and Tables 8-15.

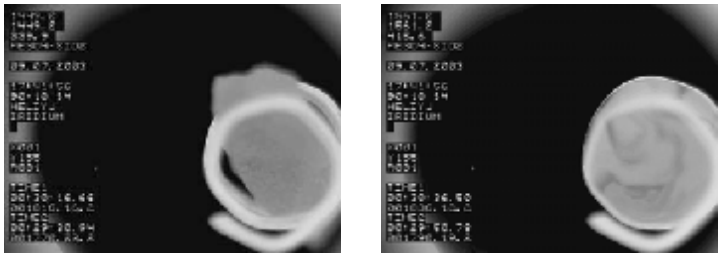

1 2

Fig. 17. Sample 1 (97 mass % Fe_3O_4**)** in the experiment with iridium holder: 1 – the beginning of melting (near solidus temperature) (T=1449.2°C); 2 – complete melting (T=1561.2°C)

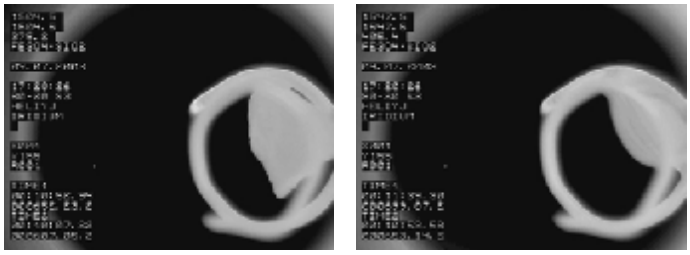

1 2

Fig. 18. Sample 2 (94 mass % Fe_3O_4**)** in the experiment with iridium holder: 1 – the beginning of melting (T=1504.5°C); 2 – complete melting (T=1547.5°C)

At the dynamic determination of the temperature and at high heating rate (~10 °C/s and higher) the temperature of the very beginning of melting process (solidus temperature) was systematically overvalued, therefore optimal heating rate was chosen as 5°C/s.

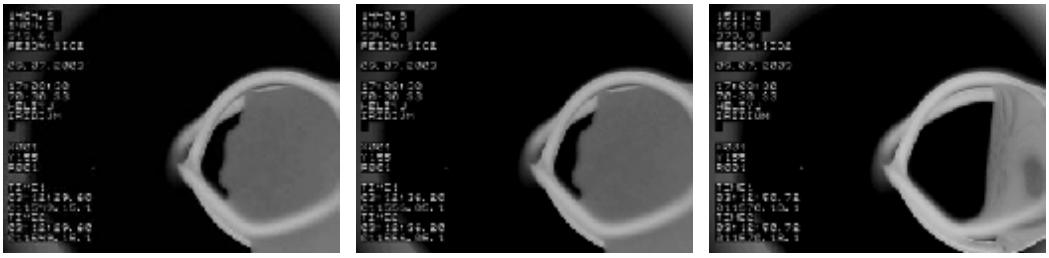

1 2 3

Fig. 19. Sample 3 (90 mass % Fe_3O_4**)** in the experiment with iridium holder: 1 – before melting (T=1404.2°C); 2 – the beginning of melting (T=1440.8°C); 3 – complete melting (T=1511.3°C)

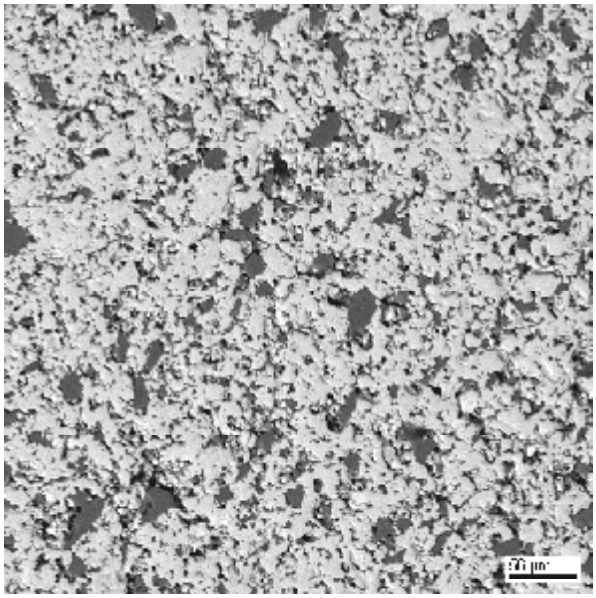

SQ

Fig. 20. Microphoto of the sample 3 (90 mass % Fe_3O_4) after preheating at 1300°C: dark domains – SiO_2 phase

Table 8

EDX-analysis results (total composition of the sample 3)

No.		Fe_3O_4	SiO_2
SQ	mass %	79.68	20.32
	mol %	50.43	49.57

From the Table 8 we can see that the total composition of the sample is rich with SiO_2 in comparison with the initial composition (Table 5). In our opinion, the reason is the surface preparing technique for analysis. During this process Fe_3O_4 grains were removed (the surface is not smooth). Therefore it is impossible to control or analyze the total composition of samples by EDX- analysis. Control was carried out by X-ray phase analysis (Fig. 11).

In addition, during the experiments at temperatures upper 1350°C (inert atmosphere, $p_{O_2} \approx 10^{-8}$) an active gas emerging was observed very likely caused by oxygen removal from Fe_3O_4 and FeO formation. This conclusion is in agreement with [8]. This circumstance may affect the measuring results of total compositions.

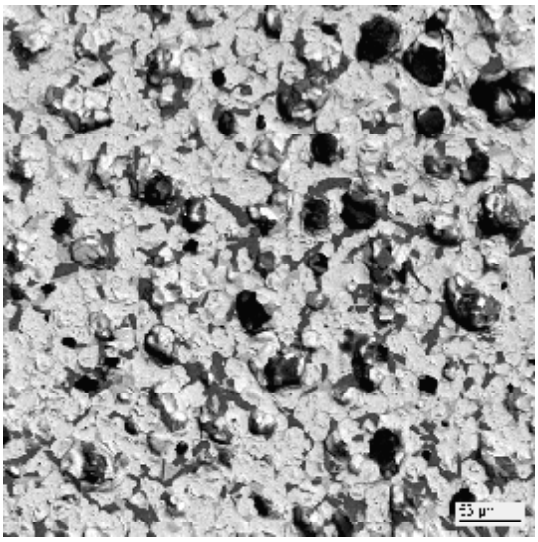

Fig. 21. Microphoto of the sample 6 (88 mass % Fe_3O_4) after preheating at 1300°C: dark domains – SiO_2 phase

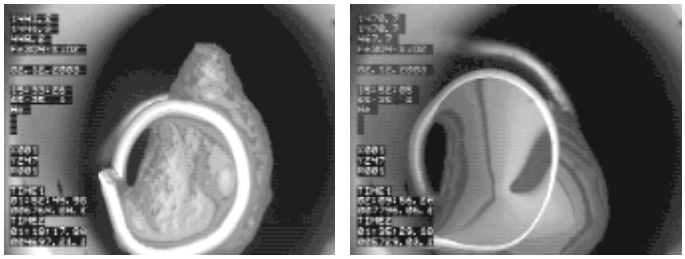

1 2

Fig. 22. Sample 6 (88 mass % Fe_3O_4**)** in the experiment with iridium holder: 1 – the beginning of melting (T=1441.2°C); 2 – complete melting (T=1470.7°C)

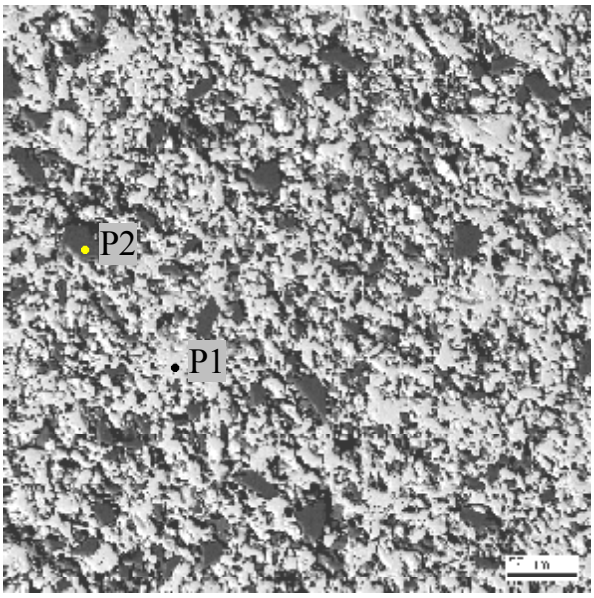

Fig. 23. Microphoto of the sample 4 (85 mass % Fe_3O_4) after preheating at 1300°C: dark domains – SiO_2 phase

Table 9

EDX-analysis results of the sample 4

No.		Fe_3O_4	SiO_2
P1	mass %	100	-
	mol %	100	-
P2	mass %	4.88	95.12
	mol %	1.31	98.69

As we can see (Table 9), the sample contained Fe_3O_4 and SiO_2 crystals (concentrations were in a good agreement with the charge compositions).

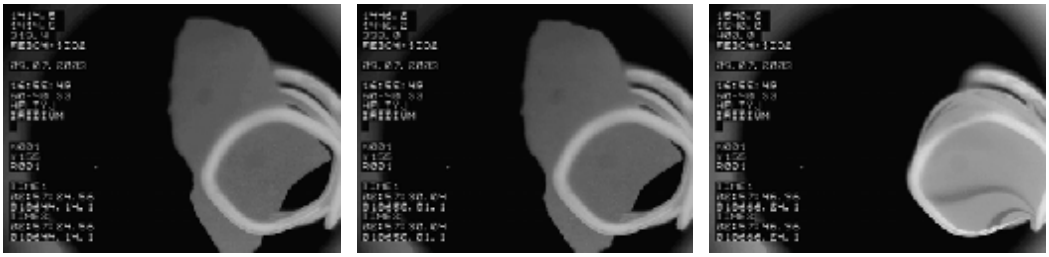

1 2 3

Fig. 24. Sample 4 (85 mass % Fe_3O_4) in the experiment with iridium holder: 1 – before melting (T=1414.5°C); 2 – the beginning of melting (T=1446.2°C); 3 – complete melting (T=1540.0°C)

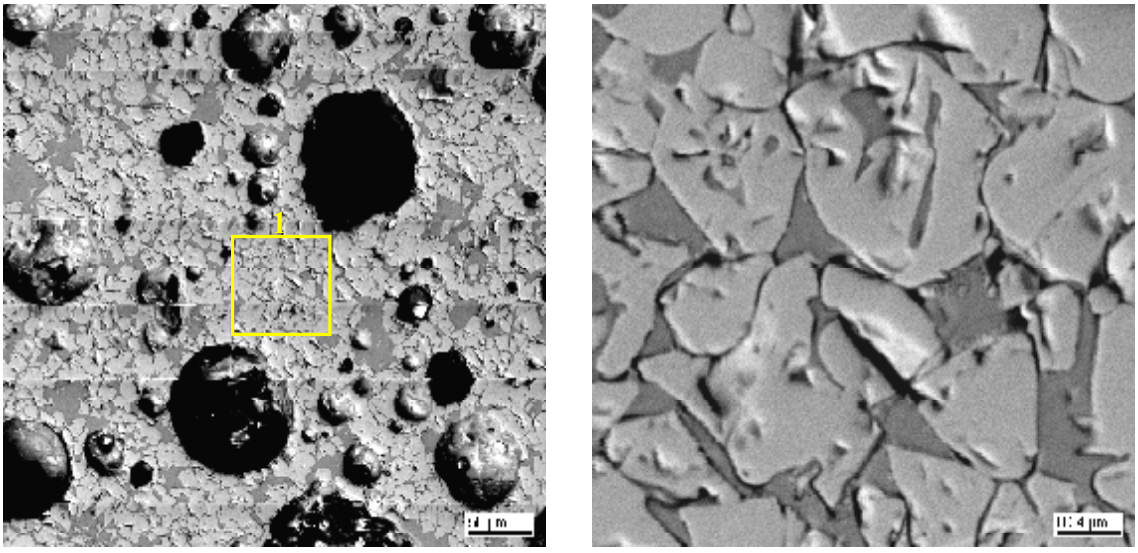

1

Fig. 25. Microphoto of the sample 4 (85 mass % Fe_3O_4) obtained by 1 min exposition at 1440°C (solidus temperature)

Microphotos (Fig. 25) represent primary crystallization domain (Fig. 16) of Fe_3O_4 phase (light phase). Due to long exposition, crystals shaped well, their polyhedral edges distinctly observed.

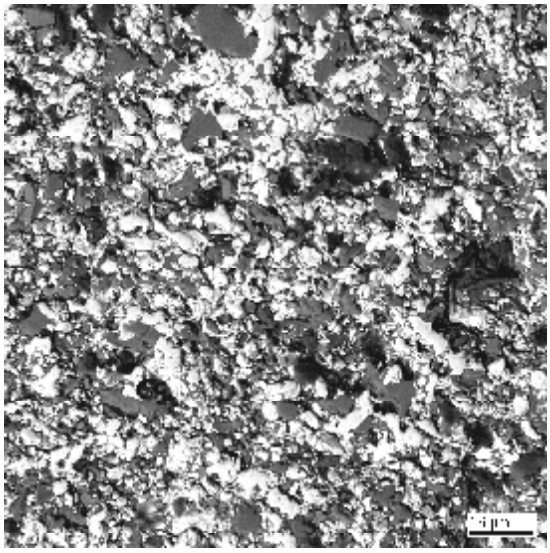

Fig. 26. Microphoto of the sample 5 (79 mass % Fe_3O_4) after preheating at 1300°C: dark domains –SiO_2 phase

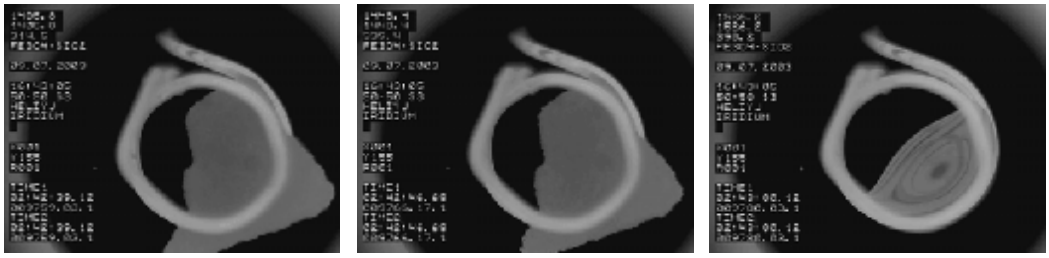

1 2 3

Fig. 27. Sample 5 (79 mass % Fe_3O_4**)** in the experiment with iridium holder: 1 – before melting (T=1405.8°C); 2 – the beginning of melting (T=1448.4°C); 3 – complete melting (T=1526.2°C)

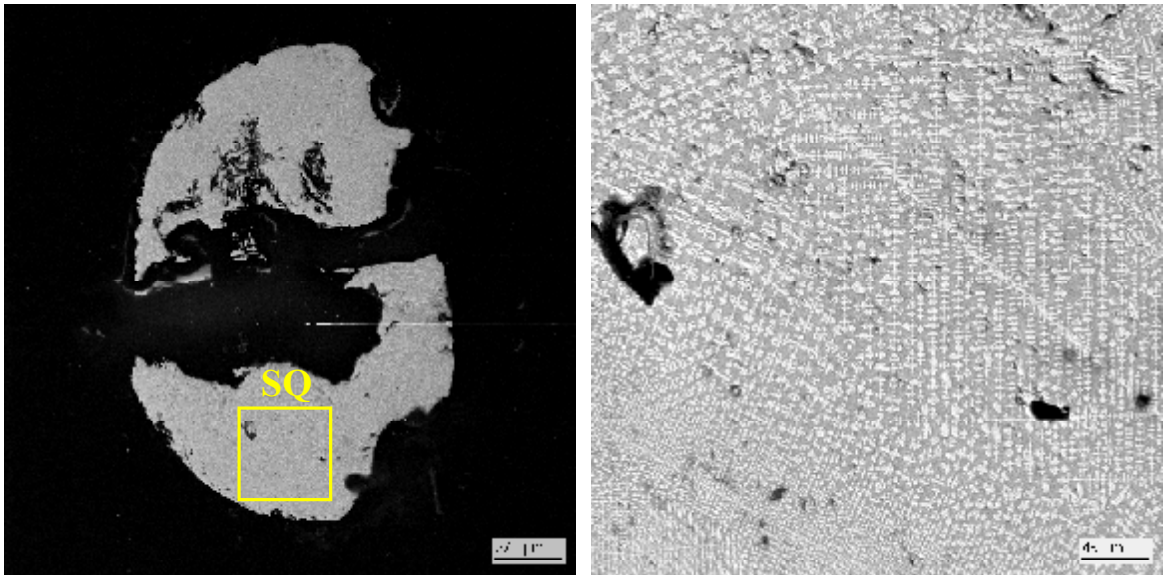

Fig. 28. Microphoto of the sample 5 (79 mass % Fe_3O_4) obtained by 5 s exposing at 1700°C and following quenching; dark domains – SiO_2 phase

Table 10

EDX-analysis results of the sample 5 obtained by 5 s exposing at 1700°C and following quenching

No.		Fe_3O_4	SiO_2
SQ	mass %	75.07	24.93
	mol %	43.87	56.13

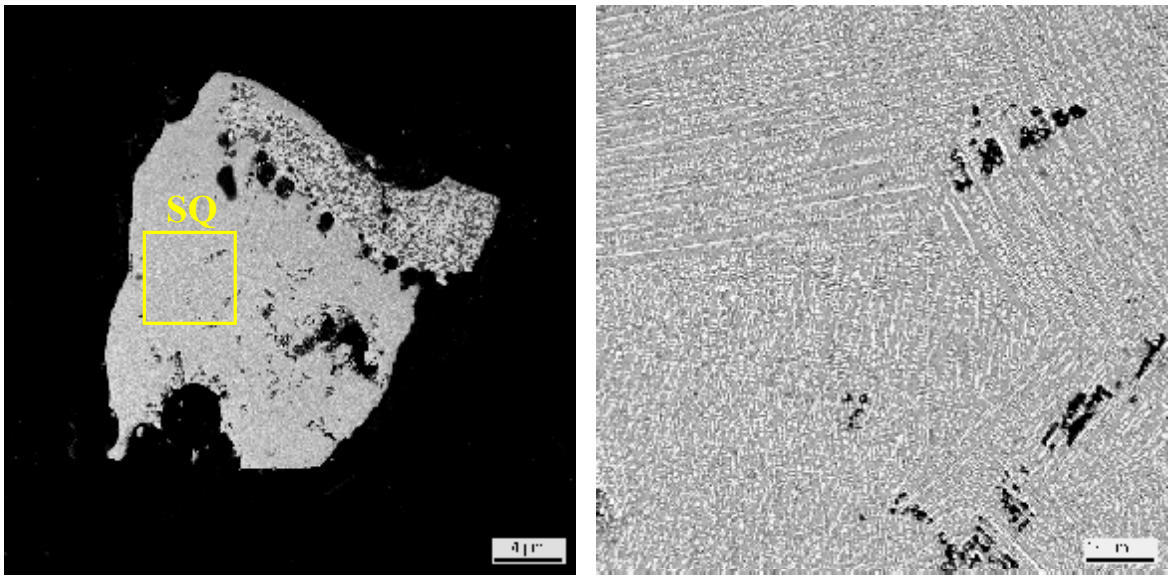

Fig. 29. Microphoto of the sample 5 (79 mass % Fe_3O_4) obtained by 7 s exposing at 1570°C and following quenching; dark domains – empty space

Table 11

EDX-analysis results of the sample 5 obtained by 7 s exposing at 1570°C and following quenching

No.		Fe_3O_4	SiO_2
SQ	mass %	74.56	25.44
	mol %	43.19	56.81

Microphotos (Fig. 28, 29) represent crystallization of both of Fe_3O_4 and SiO_2 phases very close to eutectic crystallization. Some difference in content compared to initial composition (Tables 10, 11) may be caused by oxygen loss during the heating and melting process, and as consequence, FeO formation.

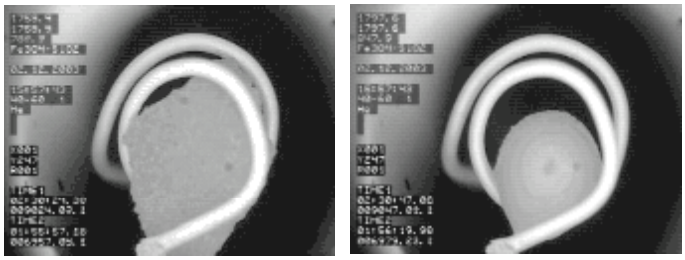

1 2

Fig. 30. Sample 7 (72 mass % Fe_3O_4**)** in the experiment with iridium holder: 1 – the beginning of melting (solidus temperature) (T=1424.7°C); 2 – complete melting (T=1797.6°C)

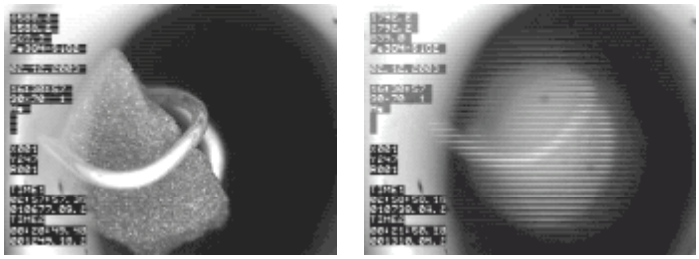

1 2

Fig. 31. Sample 8 (62 mass % Fe_3O_4**)** in the experiment with iridium holder: 1 – the beginning of active melting (T=1739.4°C); 2 – quenching (T=1792.2°C)

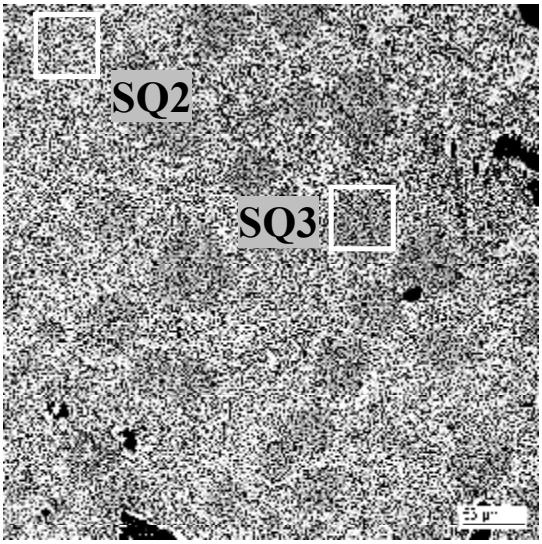

SQ1

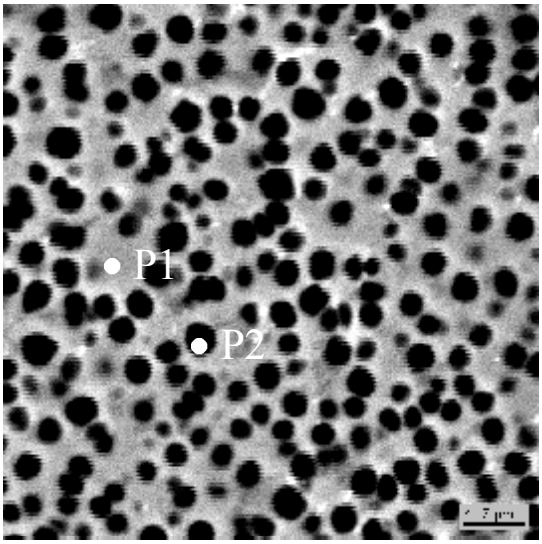

SQ2

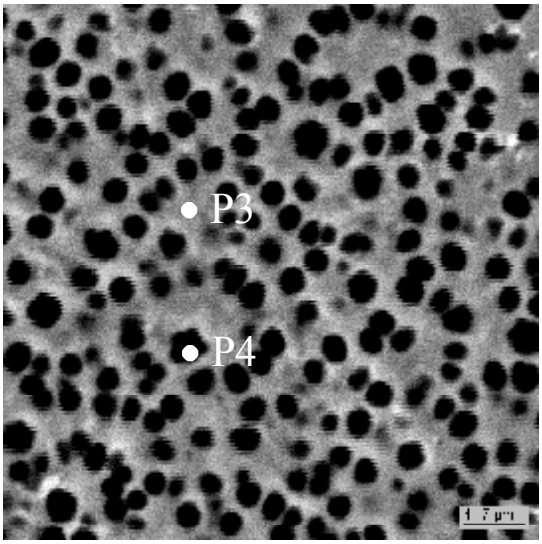

SQ3

Fig. 32. Microphoto of the sample 8 (62 mass % Fe_3O_4) obtained by 10 s exposing at 1780°C and following quenching

Table 12
EDX-analysis results of the sample 8 (62 mass % Fe_3O_4) obtained by 10 s exposing at 1780°C and following quenching

No.		Fe_3O_4	SiO_2
SQ1	mass %	52.78	47.22
	mol %	22.48	77.52
SQ2	mass %	54.47	45.53
	mol %	23.69	76.31
P1	mass %	60.99	39.01
	mol %	28.86	71.14
P2	mass %	41.38	58.62
	mol %	15.48	84.52
SQ3	mass %	48.85	51.15
	mol %	19.86	80.14
P3	mass %	58.73	41.27
	mol %	26.97	73.03
P4	mass %	43.13	56.87
	mol %	16.44	83.56

Microphotos (Fig. 32) represent miscibility gap domain at the temperature of the experiment (1780°C). The both liquids concentration was determined by EDX-analysis of marked areas (Fig. 32, Table 12).

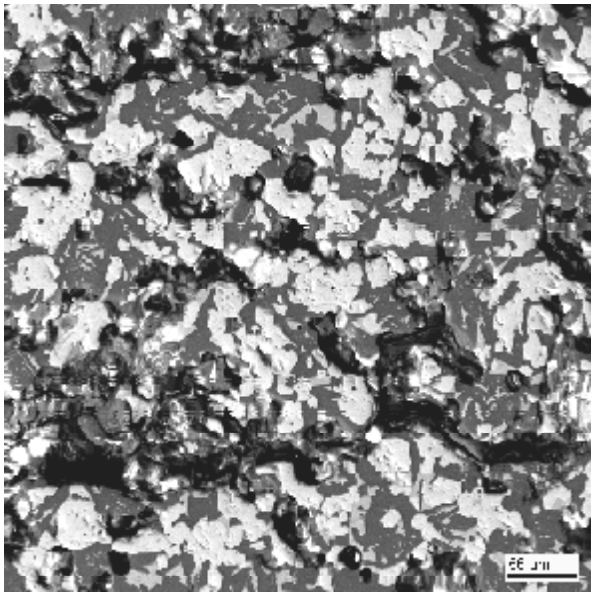

Fig. 33. Microphoto of the sample 9 (49 mass % Fe_3O_4) after preheating at 1300°C: dark domains – SiO_2 phase

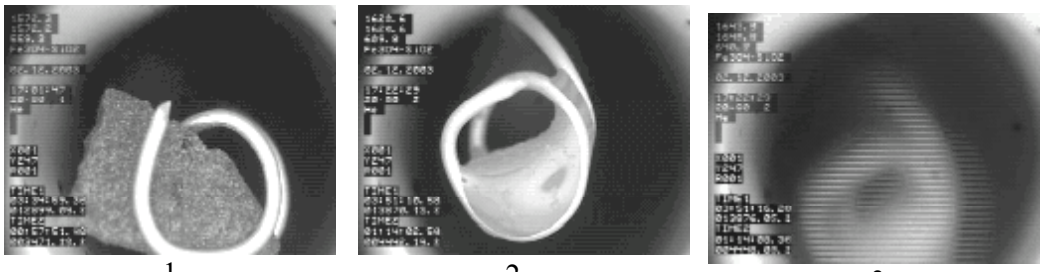

1 2 3

Fig. 34. Sample 9 (49 mass % Fe_3O_4) in the experiment with iridium holder: 1 – the beginning of melting (T=1572.2°C); 2 – complete melting (T=1620.6°C); 3 – quenching (T=1650°C)

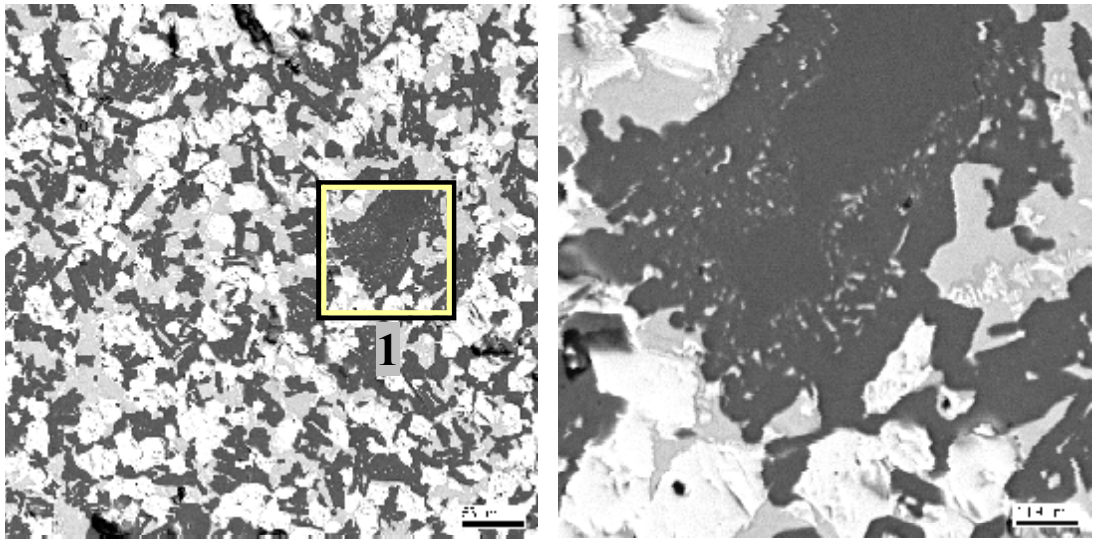

1

Fig. 35. Microphoto of the sample 9 (49 mass % Fe_3O_4) obtained by 1 min exposing at 1440°C and following quenching; dark domains – SiO_2 phase

At this temperature (1440°C) the sample began to melt down. It is well noticeable how the domains of both phases get consolidated due to separate grains association.

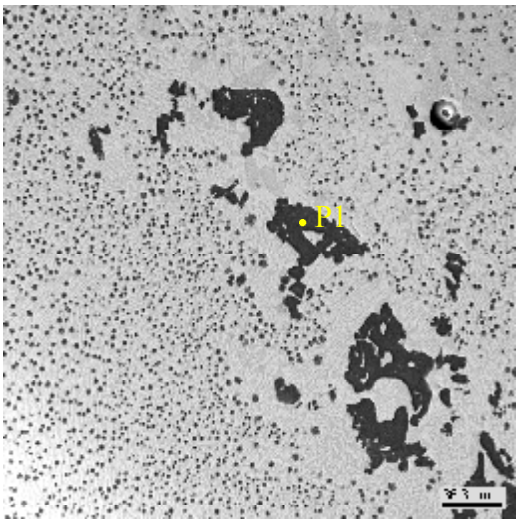

Fig. 36. Microphoto of the sample 9 (49 mass % Fe_3O_4) obtained by 1 min exposing at 1550°C and following quenching; dark domains – SiO_2 phase

At monotectic temperature (1550°C) a miscibility process was at the very beginning. Large fragments of SiO_2 phase were still observed that was evidence of EDX-analysis results (Table 13) of P1 area (Fig. 36).

Table 13

EDX- analysis results of the sample 9 obtained by 1 min exposing at 1550°C and following quenching

No.		Fe_3O_4	SiO_2
P1	mass %	2.71	97.29
	mol %	0.72	99.28

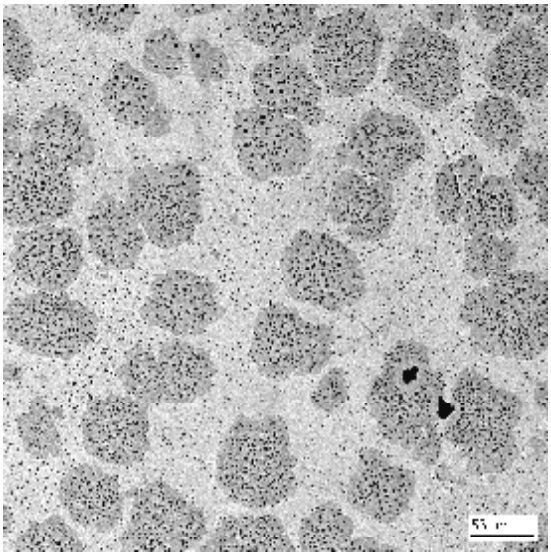

Fig. 37. Microphoto of the sample 9 (49 mass % Fe_3O_4) obtained by heating up to 1650°C and following quenching

Microphoto (Fig. 37) represents two liquids but due to high viscosity and the absence of exposition at the temperature indicated, they apparent not obviously.

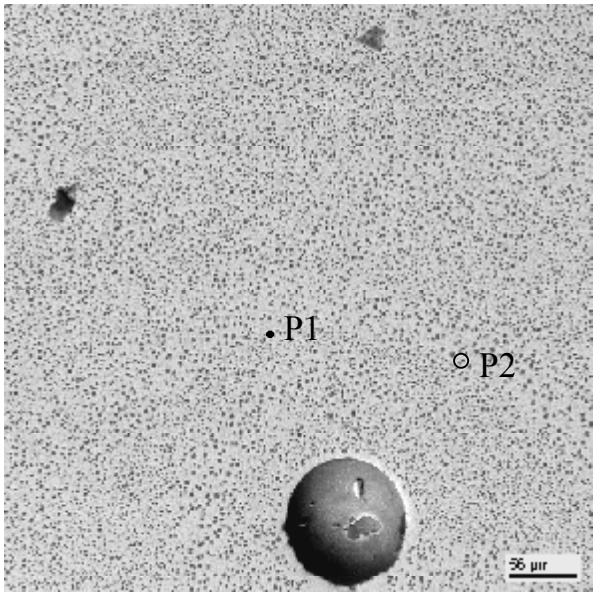

SQ

Fig. 38. Microphoto of the sample 9 (49 mass % Fe_3O_4) obtained by 1 min exposing at 1600°C and following quenching; dark round spot – pore

EDX analysis results of the total composition of the sample fragment (Fig. 38, SQ) and two liquids content (P1 and P2) are given in Table 14.

Table 14

EDX- analysis results of the sample 9 (49 mass % Fe_3O_4) obtained by 1 min exposing at 1600°C and following quenching

No.		**Fe_3O_4**	**SiO_2**
SQ	mass %	60.06	39.94
	mol %	28.07	71.93
P1	mass %	68.96	31.04
	mol %	36.57	63.43
P2	mass %	32.81	67.19
	mol %	11.25	88.75

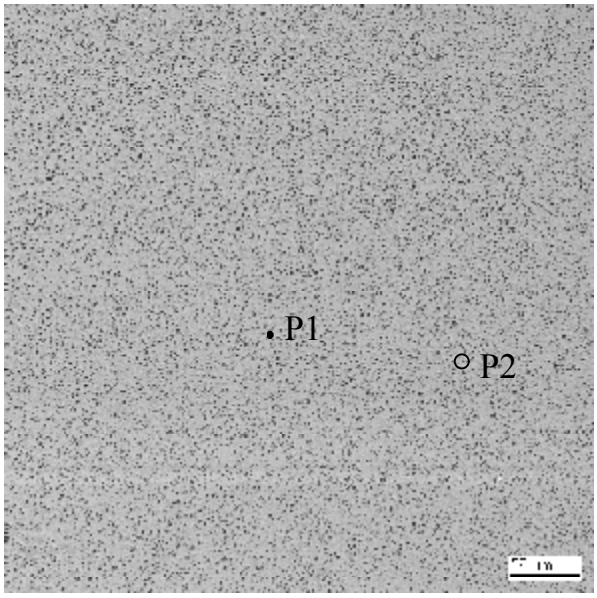

SQ

Fig. 39. Microphoto of the sample 9 (49 mass % Fe_3O_4) obtained by 1 min exposing at 1700°C and following quenching

EDX analysis results of the total composition of the sample fragment (Fig. 39, SQ) and two liquids content (P1 and P2) are given in Table 15.

Table 15

EDX- analysis results of the sample 9 (49 mass % Fe_3O_4) obtained by 1 min exposing at 1700°C and following quenching

No.		**Fe_3O_4**	**SiO_2**
SQ	mass %	61.92	38.08
	mol %	29.67	70.33
P1	mass %	67.49	32.51
	mol %	35.01	64.99
P2	mass %	42.05	57.95
	mol %	15.85	84.15

On the both of microphotos (Fig. 38, 39) two liquids are well observed. It is noticeable, that the higher is the temperature the better is two liquids distribution (more regularly).

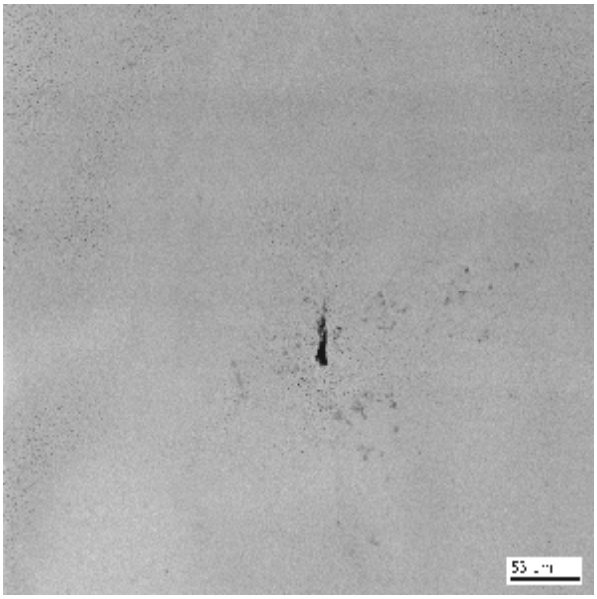

Fig. 40. Microphoto of the sample 9 (49 mass % Fe_3O_4) obtained by 1 min exposing at 2050°C and following quenching

Microphoto (Fig. 40) represents the absence of miscibility at the temperature indicated (2050°C). It gives us a possibility to determine approximately a coexistence curve location in the system.

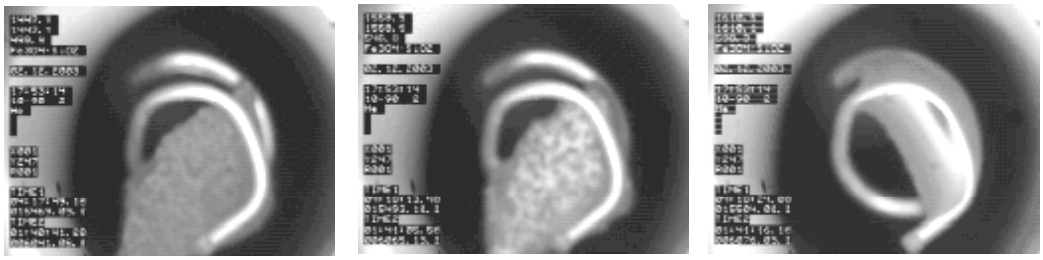

1 2 3

Fig. 41. Sample 10 (30 mass % Fe_3O_4) in the experiment with iridium holder: 1 – the beginning of melting (solidus temperature) (T=1447.1°C); 2 – the beginning of active melting (T=1559.5°C); 3 – complete melting (T=1610°C)

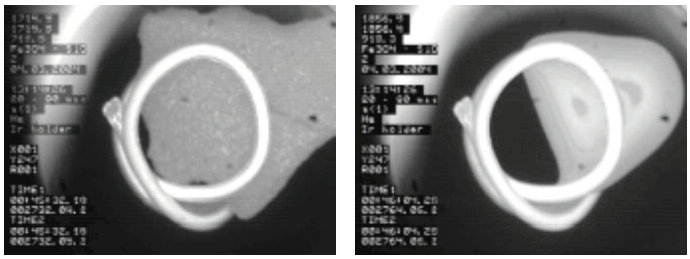

1 2

Fig. 42. Sample 13 (20 mass % Fe_3O_4) in the experiment with iridium holder: 1 – the beginning of melting (T=1715.9°C); 2 – complete melting (T=1856.4°C)

The more was silica content in the composition the more overcoming was the temperature value due to high viscosity of the melt.

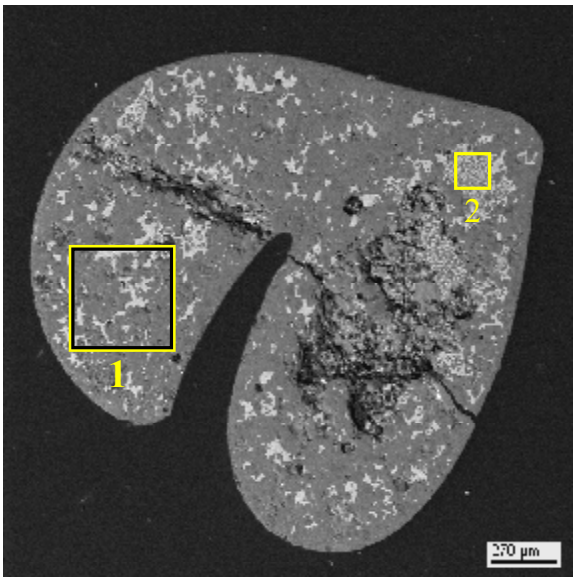

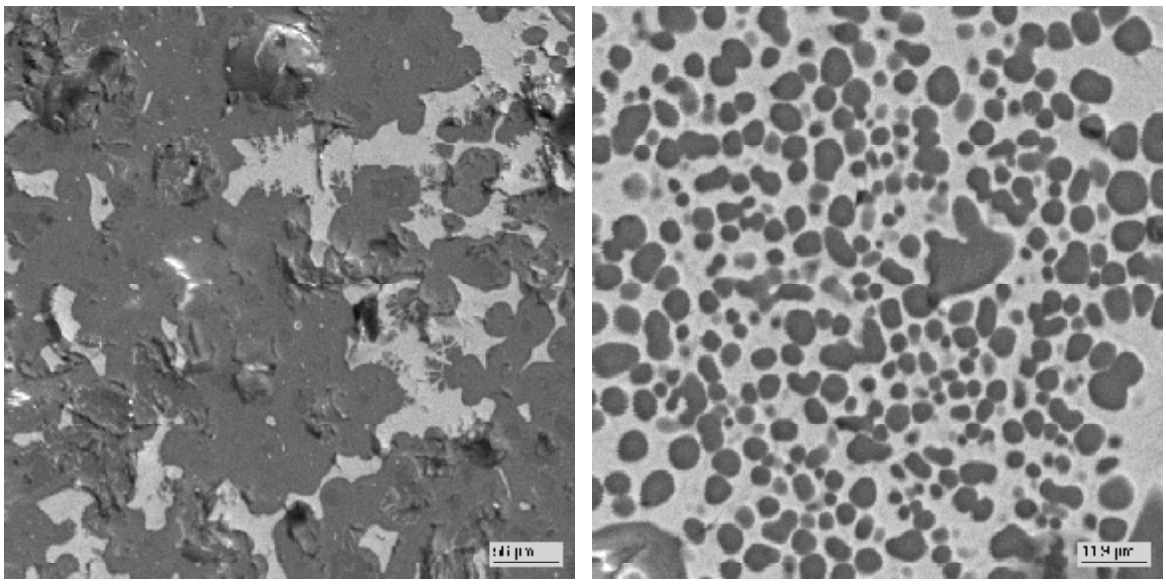

1 2

Fig. 43. Microphoto of the sample 3 (20 mass % Fe_3O_4) obtained by heating up to 1850°C, slow cooling down to 1500°C with the rate 5 °C/s and following quenching

Microphotos (Fig. 43) represent different stages of crystallization at cooling of the sample. In the temperature range from liquidus to monotectic points the primary SiO_2 crystallization was observed (dark domains on the microphoto (1)) as a glass phase at slow cooling. Below the monotectic temperature (from 1550°C to 1500°C) the combined crystallization of SiO_2 and liquid with high content of Fe_3O_4 took place. Microphoto (2) represents very likely that diphasic region located between monotectic and solidus lines (Fig. 16).

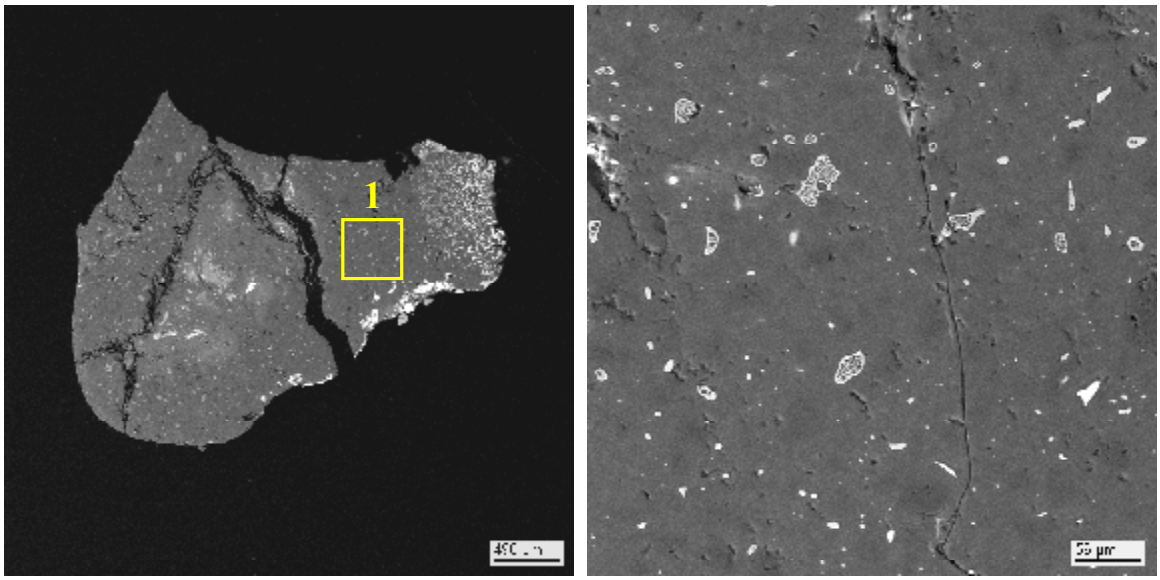

1

Fig. 44. Microphoto of the sample 3 (20 mass % Fe_3O_4) obtained by heating up to 1850°C and slow cooling with the microfurnace

The fragment marked in microphoto (Fig. 44(1)) gives a possibility to observe primary SiO_2 crystallization as supercooled melt (dark domain) with inclusions of cooled melt of higher Fe_3O_4 content at cooling from the temperature upper than liquidus point (Fig. 16).

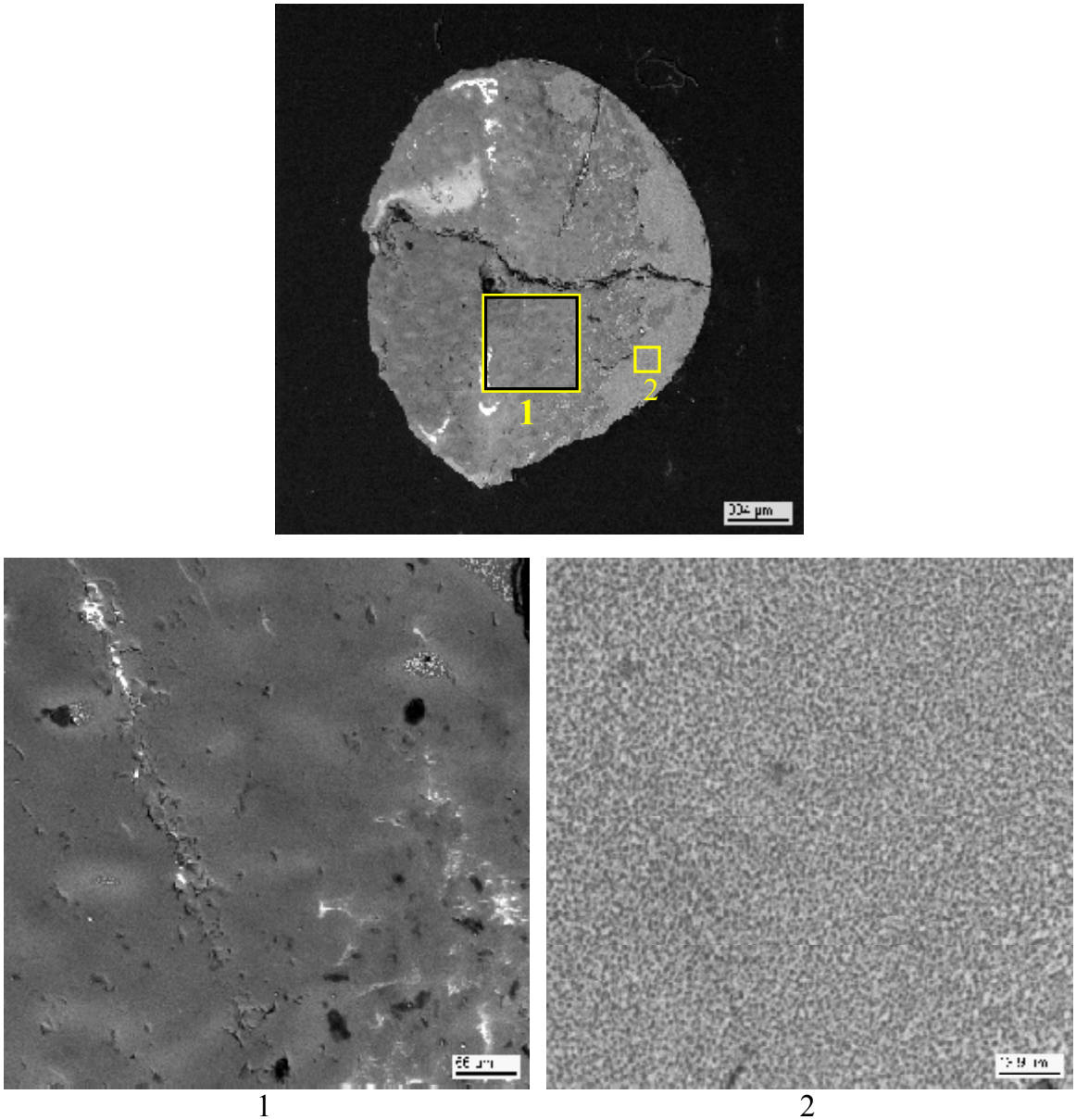

Fig. 45. Microphoto of the sample 3 (20 mass % Fe_3O_4) obtained by heating up to 2000°C and quenching

Fragments marked in microphoto represent the presence of cooled and almost homogeneous melt (Fig. 45(1)) with small inclusions of rich with Fe_3O_4 phase or partly crystallized (2) melt obtained by quenching from the temperatures significantly higher liquidus point (1720°C) of this composition.

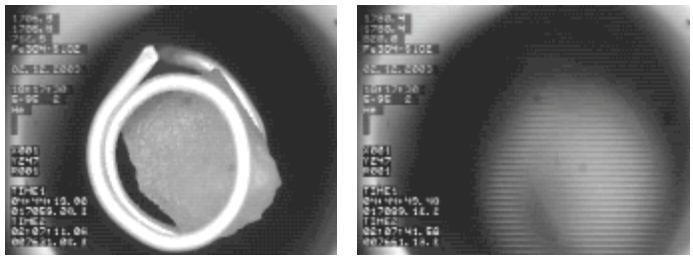

1 2

Fig. 46. Sample 11 (17 mass % Fe_3O_4) in the experiment with iridium holder: 1 – the beginning of melting (T=1706.0°C); 2 – complete melting (T=1780°C)

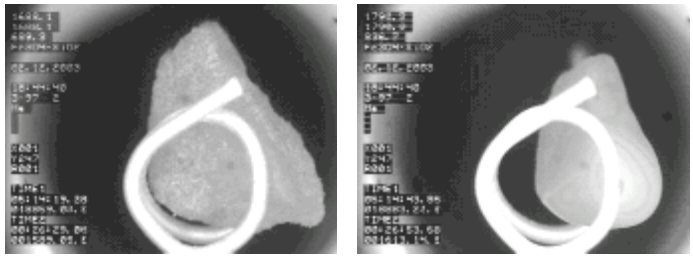

1 2

Fig. 47. Sample 12 (11 mass % Fe_3O_4) in the experiment with iridium holder: 1 – the beginning of melting (T=1688.1°C); 2 – complete melting (T=1790.0°C)

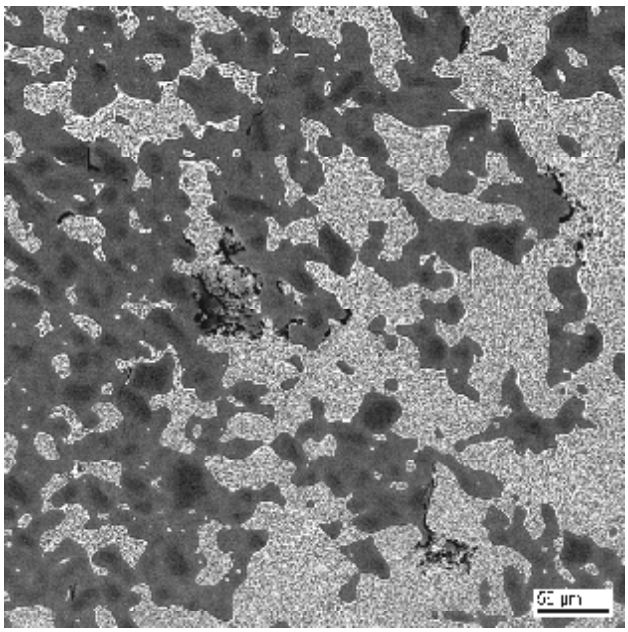

Fig. 48. Microphoto of the sample 12 (11 mass % Fe_3O_4) obtained by heating up to 1800°C and slow cooling with the microfurnace

Microphoto (Fig. 48) represents a primary SiO_2 crystallization as supercooled melt (dark domains).

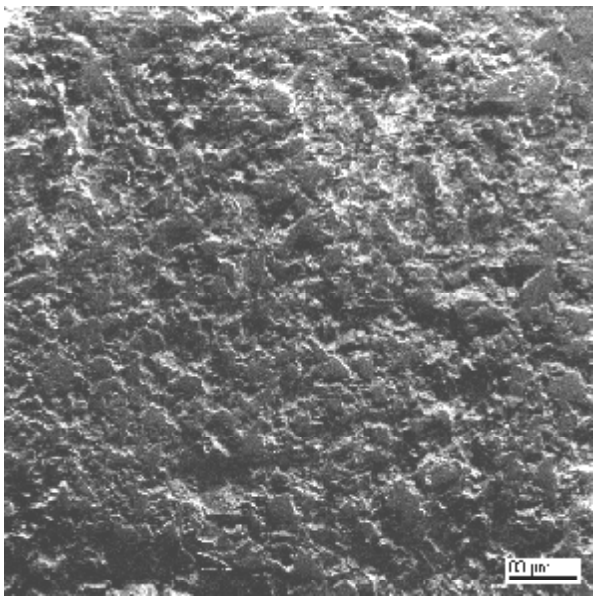

Fig. 49. Microphoto of the polished section of the sample 14 (5 mass % Fe_3O_4) after preheating at 1300°C

It is noticeable (Fig. 49) that in spite of attempts to polish thoroughly the surface it remained relief. This circumstance is one of the reasons for incorrect composition determinations of the samples after preheating at 1300°C.

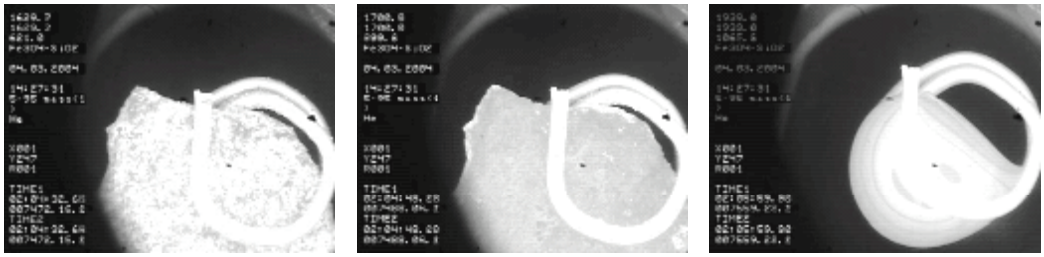

1 2 3

Fig. 50. Sample 14 (5 mass % Fe_3O_4**)** in the experiment with iridium holder: 1 – before melting (T=1629.7°C); 2 – the beginning of melting (T=1700.6°C); 3 – complete melting (T=1939.6°C)

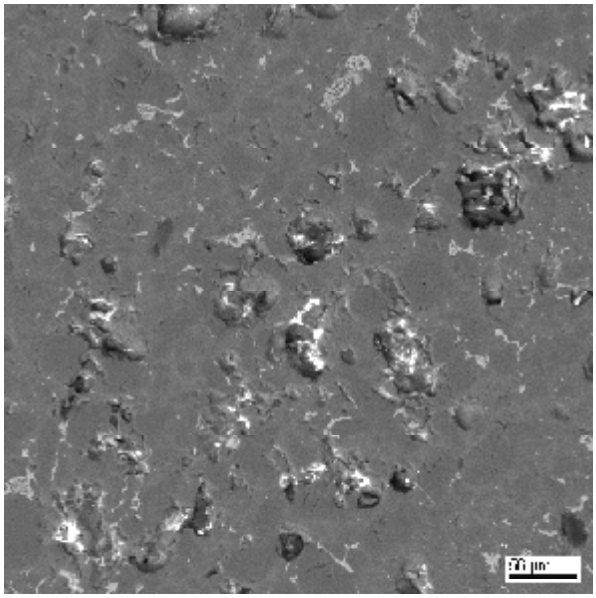

Fig. 51. Microphoto of the sample 14 (5 mass % Fe_3O_4) obtained by heating up to 1700°C and slow cooling with the microfurnace

It should be pointed out that there was not complete melting of the sample, i.e. liquidus temperature (~1710°C) was not achieved (Fig. 51).

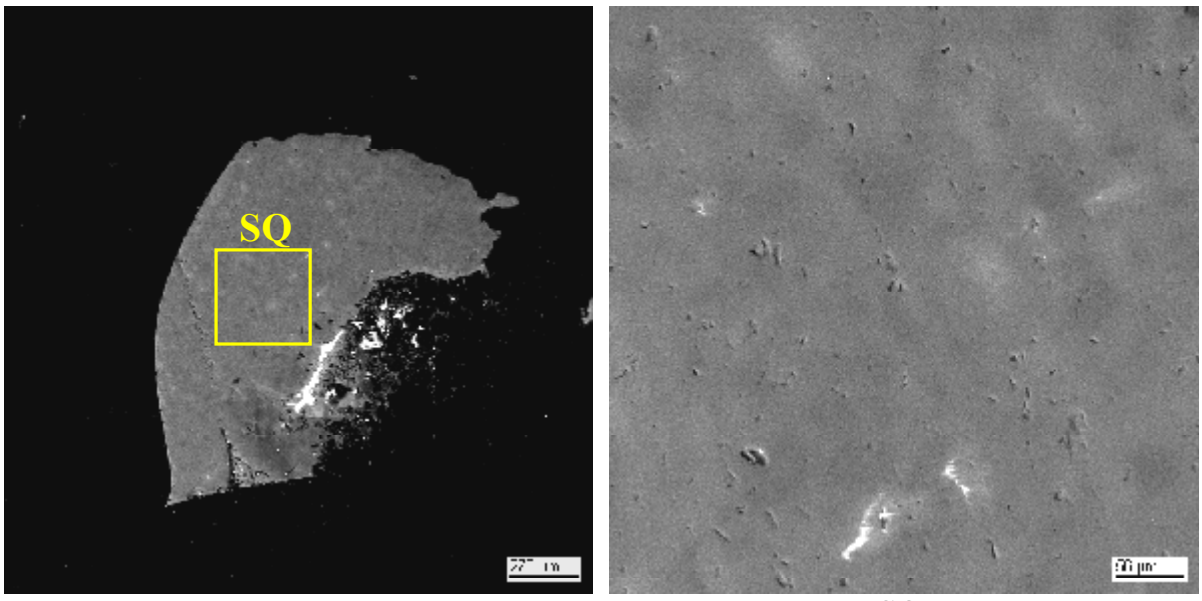

Fig. 52. Microphoto of the sample 14 (5 mass % Fe_3O_4) obtained by heating up to 1950°C, exposition 5 s with following quenching

The sample was completely melted. In the fragment of the microphoto a primary SiO_2 crystallization is shown as supercooled melt (dark domain) with inclusions of the phase based on Fe_3O_4 (light domains).

On examination the VPA results on SiO_2 containing systems the following factors are to be taken into account affected solidus-liquidus temperature determination:

- melts in such systems are particularly viscose at high SiO_2 content, therefore a liquidus temperature should be determined not according to meniscus formation which could be overvalued but to active spread beginning;
- eutectic compositions melting process is extended in time that could be due to VPA dynamic character as well as to high melt viscosity.

Combination of SEM/EDX-analysis data and VPA results has given a possibility to construct improved fusion diagram of the Fe_3O_4 – SiO_2 system (Fig. 53).

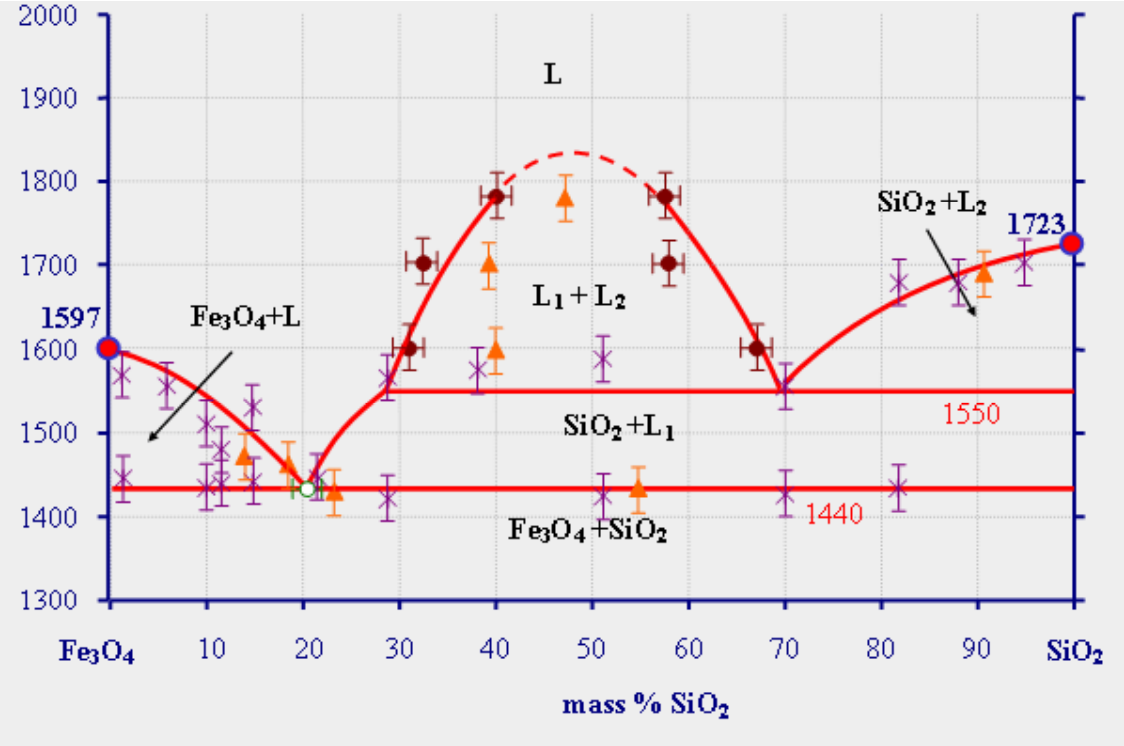

Fig. 53. Improved fusion diagram of the Fe_3O_4 – SiO_2 system (Galakhov microfurnace, inert atmosphere; $pO_2 \approx 10^{-8}$). ✳ – VPA results; ▲ – quenching; ● –SEM/EDX-analysis data on two liquids in the miscibility gap region

It is a diagram with one eutectic point at 1440°C and about 79 mass % Fe_3O_4. The region of miscibility gap extends from 70 to 30-25 mass % Fe_3O_4.

DTA analysis of the sample (49 mass % Fe_3O_4) indicated two endothermic effects (Fig. 54) - the first one at 1470°C corresponding to eutectic melting, the second one at 1550°C - to monotectic melting. These results are in a good agreement with the fusion diagram presented in Fig. 53.

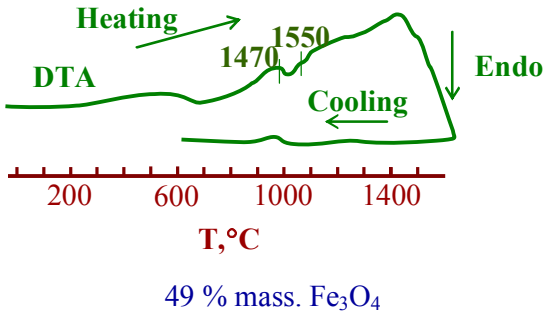

Fig. 54. DTA curves for the sample 49 mass % Fe_3O_4 in Fe_3O_4 - SiO_2 system (inert atmosphere, $p_{O_2} \approx 10^{-8}$)

2.4. Discussion of the results

Comparing the fusion diagrams (Fig. 9 and 10) of the Fe_2O_3 – SiO_2 system constructed at different oxygen partial pressure (p_{O_2}=0.21 and ~1 atm) it is possible to point out that they are almost identical. The only difference is the temperature value of Fe_2O_3 decomposition accompanying by oxygen loss and being reversible [10]. According to the present work results decomposition process take place in oxygen atmosphere at higher temperature (~50°C) compared to the experiments in air that is in a good agreement with results [10]. At upper temperature the fusion diagrams are identical. As indicated our investigations, oxygen does not affect the other processes in the system.

In the ternary Muan system [3] (Fig. 15, 55) the virtual section Fe_3O_4 – SiO_2 indicates eutectic composition in the cross point with a binary curve corresponding to 81.5 mass % Fe_3O_4. In our case it is 79±1 mass % Fe_3O_4 (Fig. 53).

According to weight loss of samples (30 mg) of Fe_2O_3 – SiO_2 system (TG curves, Fig. 6, 7 - air and oxyge) the final compositions were calculated (Table 16).

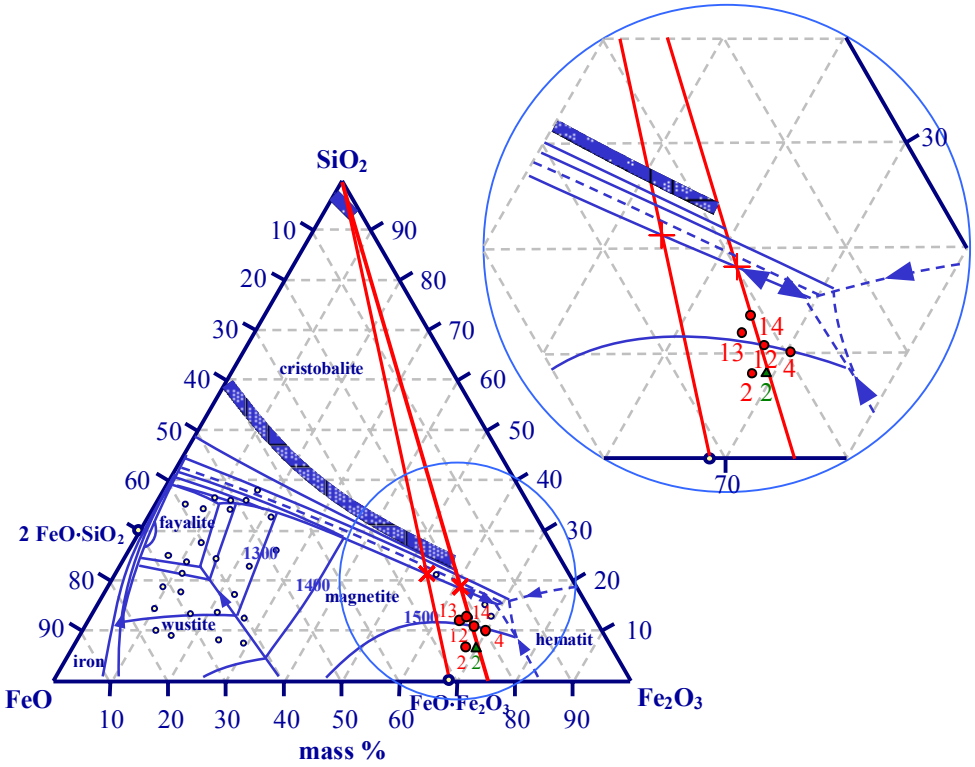

Fig. 55. Fusion diagram for the FeO – Fe_2O_3 – SiO_2 system by A. Muan [4] (mainly in reducing atmosphere) with polythermal sections of the present work

Table 16

Weight loss of samples (30 mg) of Fe_2O_3 – SiO_2 system according to DTG curves (air and oxygen atmosphere) and calculated data of final compositions

Sample number	Initial content of Fe_2O_3		Weight loss of O_2		Final Fe_2O_3 content	Theoretical* weight loss of O_2 at Fe_2O_3 decomposing	Final composition of sample		
							Fe_2O_3	FeO	SiO_2
	mass%	mg	mass%	mg	mg	mass %	mg		
2	92	27.6	2.54	0.762	7.6052	0.922	68.38	23.40	8.22
4	90	27.0	2.13	0.639	6.3776	0.902	70.23	19.55	10.22
12	89	26.7	2.37	0.711	7.0962	0.892	67.12	21.86	11.02
13	88	26.4	2.44	0.732	7.3058	0.882	65.24	22.46	12.30
14	87	26.1	2.32	0.696	6.9465	0.872	65.37	21.33	13.60
2	92 (O_2)	27.6	2.45	0.735	7.3357	0.922	69.24	22.56	8.20

* - Theoretical weight loss of O_2 calculated according a reaction $6Fe_2O_3 \rightarrow 4Fe_3O_4 + O_2$ is 3.34 mass %.

These points were plotted on the ternary Muan diagram [3] (Fig. 55: circles – air; triangle – oxygen). All of them are located outside the Fe_3O_4 – SiO_2 cross section although they contained both of Fe^{+3} and Fe^{+2}. It does mean that the figurative points of initial Fe_2O_3 – SiO_2 system corresponding to the samples heated up to the decomposition temperature of Fe_2O_3 into Fe_3O_4 shifted into the ternary diagram but did not reach though the Fe_3O_4 – SiO_2 cross section. That is why the diagrams (Fe_2O_3 – SiO_2 и Fe_3O_4 – SiO_2) are similar but not identical. Because the points of Fe_2O_3(Fe_3O_4) – SiO_2 system lied closer to ternary eutectic point predicted by A.Muan [3], liquidus temperatures in it should be lower. This is exactly what we have observed in the systems (Fig. 9, 10, 13, 54, 55). Besides, the eutectic and coexistence curve positions were somewhat different in both diagrams that agreed with the cross sections positions shown in Fig. 55.

3. Conclusions

1. The $Fe_2O_3(Fe_3O_4)$ – SiO_2 system has been investigated in air and in oxygen. Fusion diagrams of the system were constructed at different oxygen partial pressure (pO_2=0.21 and ~1 atm). It was shown that at temperatures upper 1375°C (in air) and 1430°C (in oxygen) both diagrams are identical. It is the diagrams with one eutectic point at 1440°C and 88±1 mass % of Fe_2O_3. The region of miscibility gap extends from 78/80 to ~ 20/10 mass % Fe_2O_3. The only difference is the temperature of reversible Fe_2O_3 decomposition accompanying by oxygen loss.

2. The Fe_3O_4 – SiO_2 system was investigated in inert atmosphere ($pO_2 \approx 10^{-8}$). Fusion diagram of Fe_3O_4 – SiO_2 system in inert atmosphere has been constructed. It is a diagram with one eutectic point at 1440°C and 79±1 mass % Fe_3O_4. The region of miscibility gap extends from 70 to 30 – 25 mass % Fe_3O_4.

3. Both diagrams, namely $Fe_2O_3(Fe_3O_4)$ – SiO_2 and Fe_3O_4 – SiO_2, are similar but not identical due to the incomplete reversible Fe_2O_3 decomposition into Fe_3O_4 at temperatures higher than 1375°C. This process takes place even in oxygen where it is delayed but not prevented.

References

1. Greig J.W. Am.J.Sci. 1927. V. 14. P. 474.

2. Gurry R.W., Darken L.S. The composition of CaO – FeO – Fe_2O_3 and MnO – FeO – Fe_2O_3 melts at several oxygen pressures in the vicinity of 1600°C. // J.Am.Chem.Soc. 1950. V. 72. N 9. P. 3906-3910.

3. Muan A. Phase equilibria in the system FeO – Fe_2O_3 – SiO_2.// J.Metals. 1955. N 9. P. 965-976

4. Muan A., Osborn E.F. Phase equilibria at liquidus temperature in the system MgO – FeO – Fe_2O_3 – SiO_2. // J.Am.Ceram.Soc. 1956. V. 39. N 4. P. 121-140.

5. Toropov N.A., Bondar' I.A., Lasarev A.N., Smolin Yu.I. Rare earth silicates and their analogues. Leningrad: Nauka, Leningrad Dep., 1971. – 230 p., illustr. (in Russian)

6. Galakhov F.Ya. High temperature microfurnace for heterogeneous equilibria investigations of the refractory oxides systems. – In: Modern techniques of silicates and construction materials investigation. M., 1961, P. 178-182. (in Russian)

7. Gurvich, L.V., Iorish, V.S. et al. IVTANTHERMO - A Thermodynamic Database and Software System for the Personal Computer. User's Guide. CRC Press, Inc., Boca Raton, 1993.

8. Hay R., McLeod J.M. // J.West Scotland Iron Steel Instr. 1944. V. 52. P. 109.

9. Carter P.T., Ibrahim M. // J.Soc.Glass Technol. 1952. V. 36. P. 144.

10. Hostetter J.C., Roberts H.S. J.Am.Ceram.Soc. 1921. V. 4. N 11. P. 931-950.